International Journal of Sciences: Basic and Applied Research (IJSBAR)

ISSN 2307-4531
(Print & Online)

http://gssrr.org/index.php?journal=JournalOfBasicAndApplied

Impact of Climatic Factors and Intervention Strategies on the Dynamics of Malaria in Ethiopia: A Mathematical Model Analysis

Shewakena Mersha Gebremichael[a], Temesgen Tibebu Mekonnen[b*]

[a,b]*Department of Mathematics, Debre Berhan University, Debre Berhan 445, Ethiopia*

[a]*Email: shewakenamersha@gmail.com*

[b]*Email: temesgentibebumekonnen@yahoo.com*

Abstract

In this work we considered a nonlinear dynamical system to study the impact of temperature and rainfall on the transmission of malaria disease in Ethiopia. We found disease free and endemic equilibrium points and we proved their local and global stability. We calculate the effective reproduction number using real data collected from different health sectors in Ethiopia and we found that the malaria disease spreads in both high risk and low risk areas since the effective reproduction number $\mathcal{R}_{\text{eff}}$ is greater than unity. We perform sensitivity analysis to identify the most influential control parameter of the spread of malaria disease. And thus, the most temperature dependent influential control parameter is mosquito biting rate $\epsilon(T)$ which can be controlled by insecticide treated net. The most rainfall dependent influential control parameter is larvae development rate $\xi_l(T, R)$ which can be controlled by destruction of mosquitoes breeding sites and regular use of larvicides.

KeyWords: Malaria transmission; Nonlinear dynamical system; Climatic factors; Intervention strategies; Effective reproduction number; Sensitive analysis.

1. Introduction

Malaria is a common and life-threatening infectious disease in many tropical and subtropical areas.

---

* Corresponding author.

It is caused by the Plasmodium parasite which is transmitted by female Anopheles mosquitoes while they bite humans for a blood meal for the development of their eggs [6]. The human malaria is caused by five different species of Plasmodium: Plasmodium falciparum, Plasmodium malariae, Plasmodium ovale, Plasmodium vivax and Plasmodium knowlesi. Of these, Plasmodium falciparum is the most common in tropical regions, and Plasmodium vivax in temperate zones [5, 21]. The biology of the five species of Plasmodium is generally similar and consists of two distinct phases: a sexual stage at the mosquito host and an asexual stage at the human host [13, 16, 17]. According to the World Health Organization (WHO) malaria report, nearly half of the world's population is at risk of malaria [34, 35, 36]. In 2018, an estimated 228 million cases of malaria and 405 000 deaths from malaria occurred worldwide most of which, the 93% of all malaria cases and 94% of all malaria deaths, were in the WHO African Region. The incidence rate of malaria declined globally between 2010 and 2018, from 71 to 57 cases per 1000 population at risk. However, from 2014 to 2018, the rate of change slowed dramatically, reducing to 57 in 2014 and remaining at similar levels through to 2018 [36]. Malaria is a severe disease in Ethiopia, more than 60 percent of the population lives in malarious areas, and 68 percent of the country's landmass is favorable for malaria transmission, with malaria primarily associated with altitude and rainfall [18, 19, 11, 9]. Although historically Ethiopia has been prone to periodic focal and widespread malaria epidemics, malaria epidemics have been largely absent since 2004, after the scale up of malaria control interventions [19]. However, in 2016, Public Health Emergency Management (PHEM) data have shown an increase in malaria transmission relative to previous years. According to the most recent Epidemiological Bulletin from the Ethiopian Public Health Institute (EPHI), malaria cases are trending upwards and in fact have surpassed 2014 and 2015 case levels [18]. Plasmodium *falciparum* and Plasmodium *vivax* are commonly known species in Ethiopia to cause malaria accounting for 60% and 40%, respectively [18, 11]. In order to reduce the impact of malaria in the world, many scientific efforts were done including mathematical models' construction. Mathematical models have been proposed to study the dynamics of the disease. The first model of malaria transmission was developed by Ross in 1911 [31]. According to Ross, if the mosquito population can be reduced to below a certain threshold, then malaria can be eradicated. Later, Macdonald [22] modified Ross's model by integrating biological information of latency in the mosquito due to malaria parasite development. Further extension was described by Anderson and May in 1991 [4], where the latency of infection in humans was introduced by making the additional exposed class in humans. The basic reproductive rate for this model is further reduced due to inclusion of human latency period. According to a review in [23], all other models those exist for malaria dynamics are developed from the three basic models explained earlier by incorporating different factors to make them biologically more realistic in explaining disease prevalence and prediction. Recent works have shown that the age structure of vector population and the climate effects are very important factors on the dynamics of malaria transmission because the dynamics of vector population and the biting rate from mosquitoes to humans are greatly influenced by environmental and climatic factors [6]. Moreover, in most mathematical models, the mosquito life cycle is generally ignored because eggs, larvae, and pupae are not involved in the transmission cycle. That is a useful simplification of the system but unfortunately the results of these models do not predict malaria intensity in most endemic regions. Thus, it is necessary to consider the life cycle of mosquitoes and the seasonality effect, which are very important aspects of the dynamics of malaria transmission. Our model starts from the model in [2] which is developed and analyzed by Gbenga J. Abiodun, P. Witbooi and Kazeem O. Okosun in 2018. It is a climate-based mathematical model that investigates the impact

of temperature and rainfall on malaria transmission. The main differences of our model, from that of in [2] is that, in our model we included the life cycle of vector population in the aquatic stages of the mosquito; eggs, larvae, and pupae in order to examine the influence of climatic factors on the dynamics of malaria transmission even though they are not directly involved in the transmission cycle. We also included the protected group of human population in order to measure the effect of intervention mechanisms like insecticide treated nets (ITNs), indoor residual spraying (IRS). Thus, our model is formulated as a non-autonomous system of differential equations which incorporates variability in temperature and rainfall in the life cycle of vector population and on the biting rate and mortality rate of female Anopheles mosquitoes. Then we first define a feasible region Γ in the region $\mathbb{R}_+^{10}$ where the model is epidemiologically and mathematically well-posed. Next, we prove the existence and stability of disease-free equilibrium point $\mathcal{E}_0$, through rigorous analysis of dynamical system using theories and methods. We derive the epidemic threshold parameter $\mathcal{R}_{\text{eff}}$ for predicting disease persistence using the next generation operator approach. We proved that a positive endemic equilibrium point $\mathcal{E}^*$ exists for all $\mathcal{R}_{\text{eff}} > 1$ and we explore the local and global stability of the endemic equilibrium state. Numerical simulations and sensitivity analysis of the model are also performed using the base line parameter values obtained from the data collected from the country- and world-wide sources.This paper is organized as follows. In Section 2, we formulate the mathematical model of our problem. Section 3 provides the mathematical analysis of the model. Computational simulations are performed in Section 4 in order to illustrate our mathematical results. In section 5 we include results and discussions and in the last section, section 6, we conclude and give some remarks and future works.

2. The Mathematical Model

The human population denoted by N_h is divided into five epidemiological categories the susceptible class (S_h), the protected class (P_h), the exposed class (E_h), the infectious class (I_h), and the recovered class (R_h). We also divide the mosquito population also into two major stages: the mature stage and the aquatic stage. The immature stage is divided into three compartments: eggs class E, larvae class L and pupae class P. The mature stage is divided into two compartments: the susceptible class S_v and the infectious class I_v. At any time t, the total size of humans, $N_h(t)$, and mature mosquitoes, $N_v(t)$, are respectively denoted by the following equations: $N_h(t) = S_h(t) + P_h(t) + E_h(t) + I_h(t) + R_h(t)$ and $N_v(t) = S_v(t) + I_v(t)$. It is assumed throughout this work that: all vector population measures refer to densities of female Anopheles mosquitoes, the mosquitoes bite only humans, there is no vertical transmission of malaria and all the new recruits are either susceptible or protected and no immigration considered. Using the standard incidence, we define the force of infections β_h the infection incidence from mosquitoes to humans and β_v from humans to mosquitoes, respectively as:

$$\beta_h(T) = C_{vh}\epsilon(T)\frac{I_v}{N_h} \text{ and } \beta_v(T) = C_{hv}\epsilon(T)\frac{I_h}{N_h} + \tilde{C}_{hv}\epsilon(T)\frac{R_h}{N_h}$$

2.1. Flow chart of the mathematical model

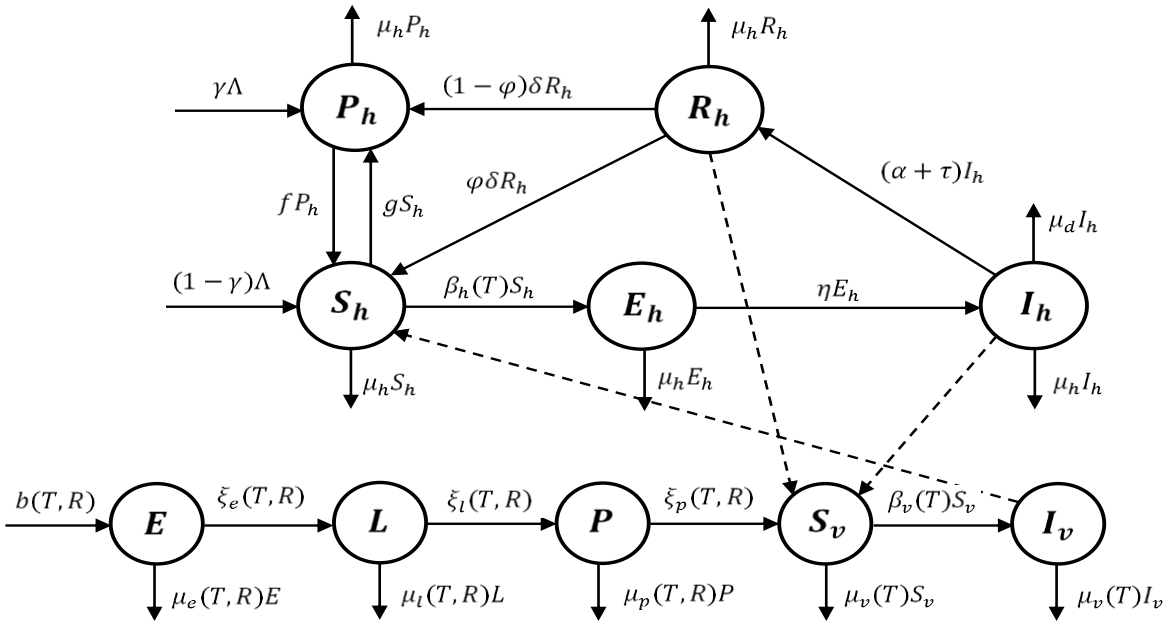

Figure 1: Flow diagram of the dynamical system (1) to (10). The dashed arrows indicate the direction of the infection and the solid arrows represent the transition from one class to another.

2.2. Dynamical system

The corresponding dynamical system of the above flow chart is the deterministic system of nonlinear differential equations [2, 1]:

$$\frac{dS_h}{dt} = (1-\gamma)\Lambda + fP_h + \varphi\delta R_h - (\beta_h + g + \mu_h)S_h \quad (1)$$

$$\frac{dP_h}{dt} = \gamma\Lambda + gS_h + (1-\varphi)\delta R_h - (f + \mu_h)P_h \quad (2)$$

$$\frac{dE_h}{dt} = \beta_h S_h - (\eta + \mu_h)E_h \quad (3)$$

$$\frac{dI_h}{dt} = \eta E_h - (\alpha + \tau + \mu_d + \mu_h)I_h \quad (4)$$

$$\frac{dR_h}{dt} = (\alpha + \tau)I_h - (\delta + \mu_h)R_h \quad (5)$$

$$\frac{dE}{dt} = b(T,R)\left(1 - \frac{E}{K_E}\right)N_v - \big(\xi_e(T,R) + \mu_e(T,R)\big)E \quad (6)$$

$$\frac{dL}{dt} = \xi_e(T,R)\left(1 - \frac{L}{K_L}\right)E - \big(\xi_l(T,R) + \mu_l(T,R)\big)L \quad (7)$$

$$\frac{dP}{dt} = \xi_l(T,R)L - \Big(\xi_p(T,R) + \mu_p(T,R)\Big)P \quad (8)$$

$$\frac{dS_v}{dt} = \xi_p(T,R)P - \big(\beta_v(T) + \mu_v(T)\big)S_v \quad (9)$$

$$\frac{dI_v}{dt} = \beta_v(T)S_v - \mu_v(T)I_v \quad (10)$$

Table 1: The State Variables and the Parameters of the model and their Descriptions.

No.	**Variables**	**Descriptions**
1	S_h	Number of Susceptible humans
2	P_h	Number of Protected humans
3	E_h	Number of Exposed humans
4	I_h	Number of Infectious humans
5	R_h	Number of Recovered humans
6	E	Eggs population
7	L	Larvae population
8	P	Pupae population
9	S_v	Number of Susceptible female mosquitoes
10	I_v	Number of Infectious female mosquitoes
No.	**Parameters**	**Descriptions**
1	Λ	Constant recruitment rate for humans
2	γ	Proportion of new recruitments that are Protected
3	g	Transfer rate of humans from Susceptible to Protected class
4	C_{vh}	Probability of transmission of infection from an infectious mosquito to a susceptible human
5	η	Rate of progression of humans from the exposed state to the infectious state
6	τ	Natural recovery rate
7	α	Recovery rate due to treatment
8	δ	Rate of loss of immunity
9	φ	Proportions of humans who lose their immunity that become Susceptible
10	f	Transfer rate of humans from Protected to Susceptible class
11	μ_h	Natural mortality rate for humans
12	μ_d	Disease-induced mortality rate for humans
13	C_{hv}	Probability of transmission of infection from an infectious human to a susceptible mosquito
14	$\tilde{C}_{hv}$	Probability of transmission of infection from a recovered human to a susceptible mosquito
15	K_E	The Eggs Carrying capacity
16	K_L	The Larvae Carrying capacity
17	$\epsilon(T)$	The mosquito biting rate
18	$\mu_v(T)$	Natural mortality rate for female mosquitoes
19	$b(T,R)$	Eggs oviposition rate
20	$\xi_e(T,R)$	Hatching rate of eggs
21	$\xi_l(T,R)$	Development rate of larvae into pupae
22	$\xi_p(T,R)$	Development rate of pupae into adult mosquitoes
23	$\mu_e(T,R)$	Natural mortality rate of eggs
24	$\mu_l(T,R)$	Natural mortality rate of larvae
25	$\mu_p(T,R)$	Natural mortality rate of pupae

3. Analysis of the Dynamical System (1) – (10)

For simplicity let $b(T,R) = b, \xi_e(T,R) = \xi_e, \xi_l(T,R) = \xi_l, \xi_p(T,R) = \xi_p, \epsilon(T) = \epsilon, \mu_h(T) = \mu_h, \mu_e(T) = \mu_e, \mu_l(T) = \mu_l, \mu_p(T) = \mu_p, \mu_d(T) = \mu_d$ *and* $\mu_v(T) = \mu_v$, and given by

Theorem 1 (Positivity of the Solutions): *If the initial values* $S_h(0) > 0$, $P_h(0) > 0$, $E_h(0) > 0$, $I_h(0) > 0$, $R_h(0) > 0$, $E(0) > 0$, $L(0) > 0$, $P(0) > 0$, $S_v(0) > 0$, *and* $I_v(0) > 0$, *then the solutions* $S_h(t)$, $P_h(t)$, $E_h(t)$, $I_h(t)$, $R_h(t)$, $E(t)$, $L(t)$, $P(t)$, $S_v(t)$ *and* $I_v(t)$ *of system* (1) to (10) *are all positive for all* $t > 0$.

Proof:

Assume that $S_h(0) > 0$, $P_h(0) > 0$, $E_h(0) > 0$, $I_h(0) > 0$, $R_h(0) > 0$, $E(0) > 0$, $L(0) > 0$, $P(0) > 0$, $S_v(0) > 0$, *and* $I_v(0) > 0$, then for all $t \geq 0$ we have to prove that $S_h(t) > 0$, $P_h(t) > 0$, $E_h(t) > 0$, $I_h(t) > 0$, $R_h(t) > 0$, $E(t) > 0$, $L(t) > 0$, $P(t) > 0$, $S_v(t) > 0$, *and* $I_v(t) > 0$. All the equations in the dynamical system are first order linear ordinary differential equations. By finding their corresponding integrating factor we found their solutions as follows

$$S_h(\bar{t}) = H_1 S_h(0) + H_1 \int_0^{\bar{t}} exp^{\left((g+\mu_h)t + \int_0^t \beta_h(w)dw\right)}\left((1-\gamma)\Lambda + fP_h(t) + \varphi\delta R_h(t)\right)dt > 0$$

$$P_h(\bar{t}) = H_2 P_h(0) + H_2 \int_0^{\bar{t}} exp^{(f+\mu_h)t}[\gamma\Lambda + gS_h(t) + (1-\varphi)\delta R_h(t)]dt > 0$$

$$E_h(\bar{t}) = H_3 E_h(0) + H_3 \int_0^{\bar{t}} exp^{(\eta+\mu_h)t}\beta_h(t)S_h(t)dt > 0$$

$$I_h(\bar{t}) = H_4 I_h(0) + H_4 \int_0^{\bar{t}} exp^{(\alpha+\tau+\mu_d+\mu_h)t}\eta E_h(t)dt > 0$$

$$R_h(\bar{t}) = H_5 R_h(0) + H_5 \int_0^{\bar{t}} exp^{(\delta+\mu_h)t}(\alpha+\tau)I_h(t)dt > 0$$

$$E(\bar{t}) = H_6 E(0) + H_6 \int_0^{\bar{t}} exp^{\left((\xi_e+\mu_e)t + \int\left(\frac{bN_v(t)}{K_E}\right)dt\right)}bN_v(t)dt > 0$$

$$L(\bar{t}) = H_7 L(0) + H_7 \int_0^{\bar{t}} exp^{\left((\xi_l+\mu_l)t + \int\left(\frac{\xi_e E(t)}{K_L}\right)dt\right)}\xi_e E(t)dt > 0$$

$$P(\bar{t}) = H_8 P(0) + H_8 \int_0^{\bar{t}} exp^{(\xi_p+\mu_p)t}\xi_l L(t)dt > 0$$

$$S_v(\bar{t}) = H_9 E(0) + H_9 \int_0^{\bar{t}} exp^{(\mu_v t + \int \beta_v(t)dt)}\xi_p P(t)dt > 0$$

$$I_v(\bar{t}) = H_{10} I_v(0) + H_{10} \int_0^{\bar{t}} exp^{\mu_v t}\beta_v(t)S_v(t)dt > 0$$

By this we have shown that all the solutions of the system are positive.

Theorem 2 (Boundedness of the solutions):

The feasible region of the system of differential equations (1) to (10) given by $\Gamma =$

$$\left\{ \left(S_h(t), P_h(t),\ E_h(t), I_h(t), R_h(t), E(t), L(t), P(t), S_v(t), I_v(t)\right) \in \right.$$

$$\mathbb{R}_+^{10} \left| \begin{array}{c} N_h \le \frac{\Lambda}{\mu_h}, \\ E(t) \le K_E, L(t) \le K_L, P(t) \le \frac{\xi_l K_L}{\xi_p + \mu_p}, \\ N_v \le \frac{\xi_p K_L}{\mu_v} \end{array} \right\}$$ is positively-invariant. That is, each solution of the system (1) to (10), with initial conditions in Γ, remains there for all $t > 0$.

Proof:

Suppose the initial conditions are in Γ, that is $N_h(0) = S_h(0) + P_h(0) + E_h(0) + I_h(0) + R_h(0) \le \frac{\Lambda}{\mu_h}$, $E(0) \le K_E$, $L(0) \le K_L$, $P(0) \le \frac{\xi_l K_L}{\xi_p + \mu_p}$, and $N_v(0) = S_v(0) + I_v(0) \le \frac{\xi_p K_L}{\mu_v}$. We have $\frac{dN_h}{dt} = \Lambda - \mu_d I_h - \mu_h N_h \le \Lambda - \mu_h N_h$ implies that $\frac{dN_h}{dt} \le \Lambda - \mu_h N_h$. By separation of variables rule, the general solutions can be solved by integrating both sides of the inequality $\frac{dN_h}{\Lambda - \mu_h N_h} \le dt$ on $[0, t]$ gives $\int_0^t \frac{dN_h(w)}{\Lambda - \mu_h N_h(\mathrm{w})} \le \int_0^t dw$, solving for $N_h(t)$ we get $N_h(t) \le \frac{\Lambda}{\mu_h} - \left(\frac{\Lambda}{\mu_h} - N_h(0)\right) e^{-\mu_h t}$. Therefore, $N_h(t) \le \frac{\Lambda}{\mu_h}$, since $N_h(0) \le \frac{\Lambda}{\mu_h}$. Thus for all $t \ge 0$ we have $0 < N_h(t) \le \frac{\Lambda}{\mu_h}$ which indicates that the total human population is bounded. We have also $\frac{dN_v}{dt} = \xi_p K_L - \mu_v N_v$ by separation of variables rule we have $\frac{dN_v}{\xi_p K_L - \mu_v N_v} = dt$. Integrating both sides of the equation on $[0, t]$ gives $\int_0^t \frac{dN_v(w)}{\xi_p K_L - \mu_v N_v(\mathrm{w})} = \int_0^t dw$, solving for $N_v(t)$ we get $N_v(t) = \frac{\xi_p K_L}{\mu_v} - \left(\frac{\xi_p K_L}{\mu_v} - N_v(0)\right) e^{-\mu_h t}$. Therefore, $N_v(t) \le \frac{\xi_p K_L}{\mu_v}$, since $N_v(0) \le \frac{\xi_p K_L}{\mu_v}$. Thus, for all $t \ge 0$ we have $0 < N_v(t) \le \frac{\xi_p K_L}{\mu_v}$ which indicates that the total mosquito population is bounded. Thus, the compact set Γ is positively invariant, and then the solutions are bounded. (i.e. all solutions with initial conditions in Γ remain in Γ for all time $t > 0$).

3.1. Disease free equilibrium point.

The disease-free equilibrium point of the model (1) to (10), is obtained by setting the right-hand sides of the equations in the dynamical system equal to zero and we found $\mathcal{E}_0 = \left(S_h^0, P_h^0,\ 0, 0, 0, E^0, L^0, P^0, S_v^0, 0\right), if\ r > 1.$

where

$$S_h^0 = \frac{(f+(1-\gamma)\mu_h)\Lambda}{(f+g+\mu_h)\mu_h}, \quad P_h^0 = \frac{(g+\gamma\mu_h)\Lambda}{(f+g+\mu_h)\mu_h}, \quad S_v^0 = \frac{\xi_p}{\mu_v}\frac{\xi_l}{\xi_p+\mu_p}\left[1-\frac{1}{r}\right]\frac{K_L}{\theta_L}$$

$$E^0 = \left[1-\frac{1}{r}\right]\frac{K_E}{\theta_E}, \qquad L^0 = \left[1-\frac{1}{r}\right]\frac{K_L}{\theta_L}, \qquad P^0 = \frac{\xi_l}{(\xi_p+\mu_p)}L^0, \tag{11}$$

with

$$r = \frac{b}{(\xi_e+\mu_e)}\frac{\xi_e}{(\xi_l+\mu_l)}\frac{\xi_l}{(\xi_p+\mu_p)}\frac{\xi_p}{\mu_v}, \quad \theta_L = 1+\frac{K_L(\xi_l+\mu_l)}{K_E\xi_e} \quad and \quad \theta_E = 1+\frac{(\xi_e+\mu_e)\,(\xi_p+\mu_p)\mu_v K_E}{b\xi_l\xi_p K_L} \tag{12}$$

3.2. Effective Reproduction Number

The basic reproduction number $\mathcal{R}_0$ is defined as the average number of secondary cases produced by a typical infected individual during his or her entire life as infectious or infectious period when introduced or allowed to live in a population of susceptible [29]. Whereas the effective reproduction number $\mathcal{R}_{eff}$ measures the average number of new infectious generated by a typically infectious individual in a community when some strategies are in place; like vaccination, intervention or treatment. We shall now in our case compute the effective reproduction number $\mathcal{R}_{eff}$ of the present model using the next generation method described by Diekmann, Heesterbeek, and Metz in [10]. Now considering the system of equations $(1)\ to\ (10)$ and re-arranging the equations so that we start with infective classes, we obtained $\frac{dX}{dt} = \mathcal{F}(X) - \mathcal{V}(X)$ where $X = \left(E_h(t), I_h(t), R_h(t), S_h(t), P_h(t),\ E(t), L(t), P(t), S_v(t), I_v(t)\right)^T$ and $\mathcal{F}$ is the rate of appearance of new infections in each compartment and $\mathcal{V}(X) = \mathcal{V}^-(X) - \mathcal{V}^+(X)$ where $\mathcal{V}^+(X)$ be the transfer rate of individuals into each compartment by all other means, and $\mathcal{V}^-(X)$ be the transfer rate of individuals out of each compartment. Then we obtained the Jacobian matrices of $\mathcal{F}$ and $\mathcal{V}$ at the disease-free steady state $\mathcal{E}_0$ with (11) and (12), $\mathcal{E}_0 = \left(S_h^0, P_h^0,\ 0, 0, 0, E^0, L^0, P^0, S_v^0, 0\right)$ as $\begin{bmatrix} F & 0 \\ 0 & 0 \end{bmatrix}$ and $\begin{bmatrix} V & 0 \\ J_3 & J_4 \end{bmatrix}$ where

$$F = \begin{bmatrix} 0 & 0 & 0 & C_{vh}\epsilon\dfrac{S_h^0}{N_h^0} \\ 0 & 0 & 0 & 0 \\ 0 & 0 & 0 & 0 \\ 0 & C_{hv}\epsilon\dfrac{S_v^0}{N_h^0} & \tilde{C}_{hv}\epsilon\dfrac{S_v^0}{N_h^0} & 0 \end{bmatrix} \quad and \quad V = \begin{bmatrix} (\eta+\mu_h) & 0 & 0 & 0 \\ -\eta & (\alpha+\tau+\mu_d+\mu_h) & 0 & 0 \\ 0 & -(\alpha+\tau) & (\delta+\mu_h) & 0 \\ 0 & 0 & 0 & \mu_v \end{bmatrix}$$

Therefore, the effective reproduction number $\mathcal{R}_{eff}$ of the model is the spectral radius of the matrix FV^{-1}, that is $\mathcal{R}_{eff} = \rho(FV^{-1})$. Thus, since we are studying the effect of interventions on the generation of secondary cases, the reproduction number $\mathcal{R}_{eff}$ of the model is:

$$\mathcal{R}_{eff} = \sqrt{\left(\frac{(f+(1-\gamma)\mu_h)\mu_h}{(f+g+\mu_h)\Lambda}\frac{C_{hv}\epsilon\eta(\delta+\mu_h)+\tilde{C}_{hv}\epsilon\eta(\alpha+\tau)}{(\eta+\mu_h)(\delta+\mu_h)(\alpha+\tau+\mu_d+\mu_h)}\right)\frac{C_{vh}\epsilon}{\mu_v}\left(\frac{K_L K_E[\xi_p\xi_l\xi_e b-\mu_v(\xi_l+\mu_l)(\xi_p+\mu_p)(\xi_e+\mu_e)]}{b\mu_v(\xi_p+\mu_p)[K_E\xi_e+K_L(\xi_l+\mu_l)]}\right)}.$$

Now if we see without intervention, that means initially the entire population is susceptible and no protected class, the basic reproduction number will appear. In that case $f = 0,\ g = 0,\ \gamma = 0,\ and\ \varphi = 0$. Then the

effective reproductive number is reduced to:

$\mathcal{R}_0 = \sqrt{\left(\frac{\mu_h}{\Lambda}\frac{C_{hv}\epsilon\eta(\delta+\mu_h)+\tilde{C}_{hv}\epsilon\eta(\alpha+\tau)}{(\eta+\mu_h)(\delta+\mu_h)(\alpha+\tau+\mu_d+\mu_h)}\right)\frac{C_{vh}\epsilon}{\mu_v}\left(\frac{K_L K_E[\xi_p\xi_l\xi_e b-\mu_v(\xi_l+\mu_l)(\xi_p+\mu_p)(\xi_e+\mu_e)]}{b\mu_v(\xi_p+\mu_p)[K_E\xi_e+K_L(\xi_l+\mu_l)]}\right)}$; which is the basic reproductive number, that measures the average number of secondary infections caused by a single infective individual in totally susceptible population.

Theorem 3 (Local stability of disease-free equilibrium point): The disease-free equilibrium point of the system of ordinary differential equations (1) to (10) is locally asymptotically stable if $\mathcal{R}_{eff} < 1$ and unstable if $\mathcal{R}_{eff} > 1$.

Proof:

To show the local stability of the disease-free equilibrium point we use the method of Jacobian matrix and Routh Hurwitz stability criteria. The Jacobian of the malaria model (1) to (10) at the disease-free equilibrium point $\mathcal{E}_0 = \left(S_h^0, P_h^0, 0, 0, 0, E^0, L^0, P^0, S_v^0, 0\right)$ is $J(\mathcal{E}_0)$ and whose characteristic equation is $|J(\mathcal{E}_0) - \lambda I| = 0$ of the form:

$$\begin{vmatrix} M_1-\lambda & f & 0 & 0 & \varphi\delta & 0 & 0 & 0 & 0 & -C_{vh}\epsilon\frac{S_h^0}{N_h^0} \\ g & M_2-\lambda & 0 & 0 & (1-\varphi)\delta & 0 & 0 & 0 & 0 & 0 \\ 0 & 0 & M_3-\lambda & 0 & 0 & 0 & 0 & 0 & 0 & C_{vh}\epsilon\frac{S_h^0}{N_h^0} \\ 0 & 0 & \eta & M_4-\lambda & 0 & 0 & 0 & 0 & 0 & 0 \\ 0 & 0 & 0 & (\alpha+\tau) & M_5-\lambda & 0 & 0 & 0 & 0 & 0 \\ 0 & 0 & 0 & 0 & 0 & M_6-\lambda & 0 & 0 & b\left(1-\frac{E^0}{K_E}\right) & b\left(1-\frac{E^0}{K_E}\right) \\ 0 & 0 & 0 & 0 & 0 & \xi_e\left(1-\frac{L^0}{K_L}\right) & M_7-\lambda & 0 & 0 & 0 \\ 0 & 0 & 0 & 0 & 0 & 0 & \xi_l & M_8-\lambda & 0 & 0 \\ 0 & 0 & 0 & -C_{hv}\epsilon\frac{S_v^0}{N_h^0} & -\tilde{C}_{hv}\epsilon\frac{S_v^0}{N_h^0} & 0 & 0 & \xi_p & M_9-\lambda & 0 \\ 0 & 0 & 0 & C_{hv}\epsilon\frac{S_v^0}{N_h^0} & \tilde{C}_{hv}\epsilon\frac{S_v^0}{N_h^0} & 0 & 0 & 0 & 0 & M_{10}-\lambda \end{vmatrix} =$$

0

where $M_1 = -(g+\mu_h)$, $M_2 = -(f+\mu_h)$, $M_3 = -(\eta+\mu_h)$, $M_4 = -(\alpha+\tau+\mu_d+\mu_h)$, $M_5 = -(\delta+\mu_h)$, $M_6 = -b\frac{S_v^0}{K_E} - (\xi_e+\mu_e)$, $M_7 = -\frac{\xi_e}{K_L}E^0 - (\xi_l+\mu_l)$, $M_8 = -\left(\xi_p+\mu_p\right)$, $M_9 = -\mu_v$, $M_{10} = -\mu_v$. And this gives an equation

$$[(M_1-\lambda)(M_2-\lambda)-fg]\left[(M_3-\lambda)(M_4-\lambda)(M_5-\lambda)(M_{10}-\lambda) - \eta C_{vh}\epsilon\frac{S_h^0}{N_h^0}\left[(\alpha+\tau)\tilde{C}_{hv}\epsilon\frac{S_v^0}{N_h^0} - (M_5-\lambda)C_{hv}\epsilon\frac{S_v^0}{N_h^0}\right]\right]\left[(M_6-\lambda)(M_7-\lambda)(M_8-\lambda)(M_9-\lambda) - \xi_e\xi_l\xi_p b\left(1-\frac{E^0}{K_E}\right)\left(1-\frac{L^0}{K_L}\right)\right] = 0$$

Using the Routh-Hurwitz stability criterion we prove that when $\mathcal{R}_{eff} < 1$ all roots of the polynomial equations

have negative real parts. Thus, the disease-free equilibrium point $\mathcal{E}_0$ is locally asymptotically stable if $\mathcal{R}_{eff} < 1$.

Theorem 4 (Global stability of the disease-free equilibrium point): For system (1) to (10), the disease-free equilibrium $\mathcal{E}_0$ is globally asymptotically stable in the feasible region Γ if $\mathcal{R}_{eff} < 1$.

Proof:

To prove the global asymptotic stability of the disease-free equilibrium $\mathcal{E}_0$ we use the method of Lyapunov functions. Technically we defined a Lyapunov function V such that;

$$V = a_1 E_h + a_2 I_h + a_3 R_h + a_4 I_v$$

where a_i ; $i = 1, 2, 3, 4$ are positive constants to be determined. Then the time derivative of V is given by

$$\frac{dV}{dt} = a_1 \frac{dE_h}{dt} + a_2 \frac{dI_h}{dt} + a_3 \frac{dR_h}{dt} + a_4 \frac{dI_v}{dt} \tag{13}$$

By substituting expressions for $\frac{dE_h}{dt}$, $\frac{dI_h}{dt}$, $\frac{dR_h}{dt}$ and $\frac{dI_v}{dt}$ from the system (1) to (10) to equation (13) and simplifying it by collecting like terms of the equation we obtain the following:

$$\frac{dV}{dt} = (a_2\eta - a_1(\eta + \mu_h))E_h + \left[a_3(\alpha + \tau) - a_2(\alpha + \tau + \mu_d + \mu_h) + a_4 C_{hv}\epsilon \frac{S_v}{N_h}\right] I_h + \left[a_4 \tilde{C}_{hv}\epsilon \frac{S_v}{N_h} - a_3(\delta + \mu_h)\right] R_h + a_1 C_{vh}\epsilon \frac{I_v}{N_h} S_h - a_4 \mu_v I_v$$

Take the coefficients of E_h, I_h, R_h are equal to zero we get $\frac{dV}{dt} = a_1 C_{vh}\epsilon \frac{I_v}{N_h} S_h - a_4 \mu_v I_v$ with

$$a_1 = \frac{\eta}{\eta + \mu_h} a_2 \text{ , } a_3(\alpha + \tau) - a_2(\alpha + \tau + \mu_d + \mu_h) + a_4 C_{hv}\epsilon \frac{S_v}{N_h} = 0 \ and \ a_3 = \frac{\tilde{C}_{hv}\epsilon \frac{S_v}{N_h}}{\delta + \mu_h} a_4 \text{ .}$$

By substituting these coefficients of $\frac{dV}{dt}$, and since $S_h \le S_h^0 \ and \ S_v \le S_v^0 \ and \ when \ N_h = N_h^0 = \frac{\Lambda}{\mu_h}$ the equation becomes;

$$\frac{dV}{dt} \le a_4 \mu_v \left[\left[\frac{\tilde{C}_{hv}\epsilon(\alpha+\tau)\eta + C_{hv}\epsilon(\delta+\mu_h)\eta}{\mu_v(\eta+\mu_h)(\delta+\mu_h)(\alpha+\tau+\mu_d+\mu_h)} \frac{(f+(1-\gamma)\mu_h)}{(f+g+\mu_h)}\right] C_{vh}\epsilon \frac{\mu_h S_v^0}{\Lambda} - 1\right] I_v = \left[{\mathcal{R}_{eff}}^2 - 1\right] I_v$$

$$where \ a_4 = \frac{1}{\mu_v},$$

Therefore, if $\mathcal{R}_{eff} \le 1$, then $\left[{\mathcal{R}_{eff}}^2 - 1\right] I_v \le 0$, so we obtain $\frac{dV}{dt} \le 0$. Furthermore, $\frac{dV}{dt} = 0$ only if $I_v = 0$ which leads to $S_v = S_v^0$, $I_h = 0$, $R_h = 0$, $E_h = 0$, $P = P^0$, $L = L^0, E = E^0$, and also leads to $S_h = S_h^0$, $P_h = P_h^0$. Thus, V is the Lyapunov function on Γ and the largest compact invariant set in $\left\{\left(S_h(t), P_h(t), E_h(t), I_h(t), R_h(t), E(t), L(t), P(t), S_v(t), I_v(t)\right) \in \Gamma: \frac{dV}{dt} = 0\right\}$ is the singleton $\{\mathcal{E}_0 =$

$\left(S_h^0, P_h^0,\ 0, 0, 0, E^0, L^0, P^0, S_v^0, 0\right)\}$. Hence by LaSalle's invariance principle [20], every solution to equations of the model (1) to (10) with initial conditions in Γ approaches the disease free equilibrium as time(t) tends to infinity $(t \to \infty)$ whenever $\mathcal{R}_{eff} \leq 1$. Hence the disease-free equilibrium is globally asymptotically stable in Γ if $\mathcal{R}_{eff} < 1$.

3.3. Existence of Endemic equilibrium point

Endemic equilibrium points are steady-state solutions where the disease persists in the population (that is, equilibria where at least one of the infected components in the model is non-zero). For our model we found an explicit representation of the endemic equilibrium point $\mathcal{E}^* = (S_h^*, P_h^*, E_h^*, I_h^*, R_h^*, E^*, L^*, P^*, S_v^*, I_v^*)$ for $\mathcal{R}_{eff} > 1$ where

$$S_h^* = \frac{\Lambda(f+(1-\gamma)\mu_h)(\alpha+\tau+\mu_d+\mu_h)(\delta+\mu_h)(\eta+\mu_h)}{[\beta_h^*(f+\mu_h)+(f+g+\mu_h)\mu_h](\alpha+\tau+\mu_d+\mu_h)(\delta+\mu_h)(\eta+\mu_h)-\delta(f+\varphi\mu_h)(\alpha+\tau)\eta\beta_h^*} \quad (14)$$

$$P_h^* = \frac{\gamma\Lambda+gS_h^*+(1-\varphi)\delta R_h^*}{f+\mu_h} \quad (15)$$

$$E_h^* = \frac{\beta_h^* S_h^*}{\eta+\mu_h} \quad (16)$$

$$I_h^* = \frac{\eta}{\alpha+\tau+\mu_d+\mu_h}\frac{\beta_h^* S_h^*}{\eta+\mu_h} \quad (17)$$

$$R_h^* = \frac{(\alpha+\tau)}{\delta+\mu_h}\frac{\eta}{\alpha+\tau+\mu_d+\mu_h}\frac{\beta_h^* S_h^*}{\eta+\mu_h} \quad (18)$$

$$E^* = \frac{bK_E(\mu_v+\beta_v^*)S_v^*}{b(\mu_v+\beta_v^*)S_v^*+\mu_v K_E(\xi_e+\mu_e)} \quad (19)$$

$$L^* = \frac{\xi_e K_L E^*}{\xi_e E^*+K_L(\xi_l+\mu_l)} \quad (20)$$

$$P^* = \frac{\xi_l L^*}{\xi_p+\mu_p} \quad (21)$$

$$S_v^* = \frac{K_E K_L[\xi_e\xi_l\xi_p b-\mu_v(\xi_e+\mu_e)(\xi_l+\mu_l)(\xi_p+\mu_p)]}{b(\xi_p+\mu_p)(\mu_v+\beta_v^*)[\xi_e K_E+K_L(\xi_l+\mu_l)]} \quad (22)$$

$$I_v^* = \frac{\beta_v^* S_v^*}{\mu_v} \quad (23)$$

Theorem 5

(Local stability of endemic equilibrium point):

The endemic equilibrium $\mathcal{E}^* = (S_h^*, P_h^*, E_h^*, I_h^*, R_h^*, E^*, L^*, P^*, S_v^*, I_v^*)$ given from (14) to (23) of the system (1) to (10), is locally asymptotically stable if $\mathcal{R}_{eff} > 1$.

Proof:

To show the local stability of the endemic equilibrium point we use the method of Jacobian matrix and Routh Hurwitz stability criteria. Then the Jacobian matrix of the dynamical system (1) to (10) at the endemic equilibrium point $\mathcal{E}^* = (S_h^*, P_h^*, E_h^*, I_h^*, R_h^*, E^*, L^*, P^*, S_v^*, I_v^*)$ given from (14) to (23) is $J(\mathcal{E}^*)$ with the characteristic equation $|J(\mathcal{E}^*) - \lambda I| = 0$ can be found as follows:

$$\begin{vmatrix} Z_1-\lambda & f & 0 & 0 & \varphi\delta & 0 & 0 & 0 & 0 & -q_1 \\ g & Z_2-\lambda & 0 & 0 & (1-\varphi)\delta & 0 & 0 & 0 & 0 & 0 \\ \beta_h^* & 0 & Z_3-\lambda & 0 & 0 & 0 & 0 & 0 & 0 & q_1 \\ 0 & 0 & \eta & Z_4-\lambda & 0 & 0 & 0 & 0 & 0 & 0 \\ 0 & 0 & 0 & (\alpha+\tau) & Z_5-\lambda & 0 & 0 & 0 & 0 & 0 \\ 0 & 0 & 0 & 0 & 0 & Z_6-\lambda & 0 & 0 & q_2 & q_2 \\ 0 & 0 & 0 & 0 & 0 & q_3 & Z_7-\lambda & 0 & 0 & 0 \\ 0 & 0 & 0 & 0 & 0 & 0 & \xi_l & Z_8-\lambda & 0 & 0 \\ 0 & 0 & 0 & -q_4 & -q_5 & 0 & 0 & \xi_p & Z_9-\lambda & 0 \\ 0 & 0 & 0 & q_4 & q_5 & 0 & 0 & 0 & \beta_v^* & Z_{10}-\lambda \end{vmatrix} = 0$$

where $Z_1 = -(\beta_h^* + g + \mu_h)$, $Z_2 = -(f + \mu_h)$, $Z_3 = -(\eta + \mu_h)$, $Z_4 = -(\alpha + \tau + \mu_d + \mu_h)$, $Z_5 = -(\delta + \mu_h)$, $Z_6 = -b\frac{N_v^*}{K_E} - (\xi_e + \mu_e)$, $Z_7 = -\frac{\xi_e}{K_L}E^* - (\xi_l + \mu_l)$, $Z_8 = -(\xi_p + \mu_p)$, $Z_9 = -(\beta_v^* + \mu_v)$, $Z_{10} = -\mu_v$, $q_1 = C_{vh}\epsilon\frac{S_h^*}{N_h^*}$, $q_2 = b\left(1 - \frac{E^*}{K_E}\right)$, $q_3 = \xi_e\left(1 - \frac{L^*}{K_L}\right)$, $q_4 = C_{hv}\epsilon\frac{S_v^*}{N_h^*}$, $q_5 = \tilde{C}_{hv}\epsilon\frac{S_v^*}{N_h^*}$ and gives an equation:

$$\{[[(Z_2-\lambda)(Z_1-\lambda) - fg](Z_3-\lambda)(Z_4-\lambda)(Z_5-\lambda) + [f\beta_h^*\eta(1-\varphi)\delta - (Z_2-\lambda)\beta_h^*\eta\varphi\delta](\alpha+\tau)](Z_{10}-\lambda) + [\eta q_1[(Z_2-\lambda)(Z_1-\lambda) - fg] + (Z_2-\lambda)\beta_h^*\eta q_1][(Z_5-\lambda)q_4 - (\alpha+\tau)q_5]\}\big((Z_6-\lambda)(Z_7-\lambda)(Z_8-\lambda)(Z_9-\lambda) - q_2q_3\xi_l\xi_p\big) + [[(Z_2-\lambda)(Z_1-\lambda) - fg](Z_3-\lambda)(Z_4-\lambda)(Z_5-\lambda) + [f\beta_h^*\eta(1-\varphi)\delta - (Z_2-\lambda)\beta_h^*\eta\varphi\delta](\alpha+\tau)]\beta_v^*q_2q_3\xi_l\xi_p + [\eta q_1[(Z_2-\lambda)(Z_1-\lambda) - fg] + (Z_2-\lambda)\beta_h^*\eta q_1]\beta_v^*\big((Z_5-\lambda)q_4 - (\alpha+\tau)q_5\big)(Z_6-\lambda)(Z_7-\lambda)(Z_8-\lambda) = 0$$

$$\Rightarrow (A_4\lambda^4 + A_3\lambda^3 + A_2\lambda^2 + A_1\lambda + A_0)(a_6\lambda^6 + a_5\lambda^5 + a_4\lambda^4 + a_3\lambda^3 + a_2\lambda^2 + a_1\lambda + a_0) = 0$$

Using the Routh-Hurwitz stability criterion we prove that when $\mathcal{R}_{eff} > 1$ all roots of the polynomial equations have negative real parts. Thus, the endemic equilibrium point $\mathcal{E}^*$ is locally asymptotically stable if $\mathcal{R}_{eff} > 1$.

Theorem 6 (Global stability of endemic equilibrium point):

If $\mathcal{R}_{eff} > 1$, the endemic equilibrium $\mathcal{E}^* = (S_h^*, P_h^*, E_h^*, I_h^*, R_h^*, E^*, L^*, P^*, S_v^*, I_v^*)$ given from (14) to (23) of the model (1) to (10) is globally asymptotically stable.

Proof: First, we define an appropriate Lyapunov function V technically such that;

$$V(X) = \left(S_h - S_h^* - S_h^*\ln\left(\frac{S_h}{S_h^*}\right)\right) + \left(P_h - P_h^* - P_h^*\ln\left(\frac{P_h}{P_h^*}\right)\right) + \left(E_h - E_h^* - E_h^*\ln\left(\frac{E_h}{E_h^*}\right)\right) + \left(I_h - I_h^* - I_h^*\ln\left(\frac{I_h}{I_h^*}\right)\right) + \left(R_h - R_h^* - R_h^*\ln\left(\frac{R_h}{R_h^*}\right)\right) + \left(E - E^* - E^*\ln\left(\frac{E}{E^*}\right)\right) + \left(L - L^* - L^*\ln\left(\frac{L}{L^*}\right)\right) + \left(P - P^* -\right.$$

$$P^* \ln\left(\frac{P}{P^*}\right)\Big) + \left(S_v - S_v^* - S_v^* \ln\left(\frac{S_v}{S_v^*}\right)\right) + \left(I_v - I_v^* - I_v^* \ln\left(\frac{I_v}{I_v^*}\right)\right)$$

Then differentiating with respect to t gives,

$$\frac{dV}{dt} = \left(1 - \frac{S_h^*}{S_h}\right)\frac{dS_h}{dt} + \left(1 - \frac{P_h^*}{P_h}\right)\frac{dP_h}{dt} + \left(1 - \frac{E_h^*}{E_h}\right)\frac{dE_h}{dt} + \left(1 - \frac{I_h^*}{I_h}\right)\frac{dI_h}{dt} + \left(1 - \frac{R_h^*}{R_h}\right)\frac{dR_h}{dt} + \left(1 - \frac{E^*}{E}\right)\frac{dE}{dt} + \left(1 - \frac{L^*}{L}\right)\frac{dL}{dt} + \left(1 - \frac{P^*}{P}\right)\frac{dP}{dt} + \left(1 - \frac{S_v^*}{S_v}\right)\frac{dS_v}{dt} + \left(1 - \frac{I_v^*}{I_v}\right)\frac{dI_v}{dt}$$

Substituting the derivatives from their respective expressions in equation (1) to (10) and simplifying it by collecting like terms of the equation we obtain: $\frac{dV}{dt} = H - K$ where

$$H = \gamma\Lambda + fP_h + \varphi\delta R_h + (\beta_h + g + \mu_h)S_h^* + (1-\gamma)\Lambda + gS_h + (1-\varphi)\delta R_h + (f + \mu_h)P_h^* + \beta_h S_h + (\eta + \mu_h)E_h^* + \eta E_h + (\alpha + \tau + \mu_d + \mu_h)I_h^* + (\alpha + \tau)I_h + (\delta + \mu_h)R_h^* + b\left(1 - \frac{E}{K_E}\right)N_v + (\xi_e + \mu_e)E^* + \xi_e\left(1 - \frac{L}{K_L}\right)E + (\xi_l + \mu_l)L^* + \xi_l L + \left(\xi_p + \mu_p\right)P^* + \xi_p P + (\beta_v + \mu_v)S_v^* + \beta_v S_v + \mu_v I_v^*$$ and

$$K = (\beta_h + g + \mu_h)S_h + \frac{S_h^*}{S_h}\gamma\Lambda + \frac{S_h^*}{S_h}fP_h + \frac{S_h^*}{S_h}\varphi\delta R_h + (f + \mu_h)P_h + \frac{P_h^*}{P_h}(1-\gamma)\Lambda + \frac{P_h^*}{P_h}gS_h + \frac{P_h^*}{P_h}(1-\varphi)\delta R_h + (\eta + \mu_h)E_h + \frac{E_h^*}{E_h}\beta_h S_h + (\alpha + \tau + \mu_d + \mu_h)I_h + \frac{I_h^*}{I_h}\eta E_h + (\delta + \mu_h)R_h + \frac{R_h^*}{R_h}(\alpha + \tau)I_h + (\xi_e + \mu_e)E + \frac{E^*}{E}b\left(1 - \frac{E}{K_E}\right)N_v + (\xi_l + \mu_l)L + \frac{L^*}{L}\xi_e\left(1 - \frac{L}{K_L}\right)E + \left(\xi_p + \mu_p\right)P + \frac{P^*}{P}\xi_l L + (\beta_v + \mu_v)S_v + \frac{S_v^*}{S_v}\xi_p P + \mu_v I_v + \frac{I_v^*}{I_v}\beta_v S_v$$

Thus if $H < K$, then $\frac{dV}{dt} \leq 0$; and $\frac{dV}{dt} = 0$ if and only if $S_h = S_h^*,\ P_h = P_h^*,\ E_h = E_h^*, I_h = I_h^*,\ R_h = R_h^*, E = E^*,\ L = L^*,\ P = P^*,\ S_v = S_v^*$, and $I_v = I_v^*$. Hence V is the Lyapunov function on Γ and the set $\{\mathcal{E}^* = (S_h^*, P_h^*, E_h^*, I_h^*, R_h^*, E^*, L^*, P^*, S_v^*, I_v^*)\}$ is the largest compact invariant singleton set in $\left\{\left(S_h(t), P_h(t),\ E_h(t), I_h(t), R_h(t), E(t), L(t), P(t), S_v(t), I_v(t)\right) \in \Gamma: \frac{dV}{dt} = 0\right\}$. Therefore, by the principle of Lasalle, the endemic equilibrium $\mathcal{E}^*$, is globally asymptotically stable in the invariant region Γ if $H < K$ for $\mathcal{R}_{eff} > 1$.

3.4. Impact of Temperature and Rain Fall

3.4.1. Temperature-dependent parameters of the model

Mosquito biting rate $\epsilon(T)$: The temperature-dependent mosquito biting rate of adult female mosquito $\epsilon(T)$ is defined by the expression of [2, 24, 27] as

$$\epsilon(T) = 0.000203T(T - 11.7)\sqrt{42.3 - T} \tag{24}$$

Mosquito mortality rate $\mu_v(T)$: The temperature-dependent mortality rate $\mu_v(T)$ of adult female mosquito is defined by the expression of **[1]** as

$$\mu_v(T) = 0.0005\ (\mathrm{T} - 28)^2 + 0.04 \quad (25)$$

3.4.2. Temperature- and rainfall-dependent parameters of the model

To estimate the temperature-and rainfall-dependent parameters of aquatic stages, we adopt the expression of [1]. The parameter $b(T,R)$ for the rate of eggs laid per oviposition, is defined as

$$b(T,R) = \alpha_b u_b(T) v_b(R) \quad (26)$$

where $u_b(T)\ and\ v_b(R)$ account for the effect of temperature and rainfall, respectively, on the daily survival probability of eggs laid. The parameter α_b represents the maximum rate of eggs laid per oviposition. Similarly, the transition rates $\xi_j(T,R)$ are defined as

$$\xi_j(T,R) = \alpha_j g_j(T) h_j(R)\ ;\ j = \{E,L,P\} \quad (27)$$

Where $g_j(T)$ and $h_j(R)$ account for the effect of temperature and rainfall, respectively, on the transition rates $\xi_j(T,R)$. Furthermore, α_j represents the maximum rate of transition between the aquatic stages. The mortality rate for the three aquatic stages of the mosquito are defined as

$$\mu_j(T,R) = p_j(T) q_j(R)\ ;\ j = \{E,L,P\} \quad (28)$$

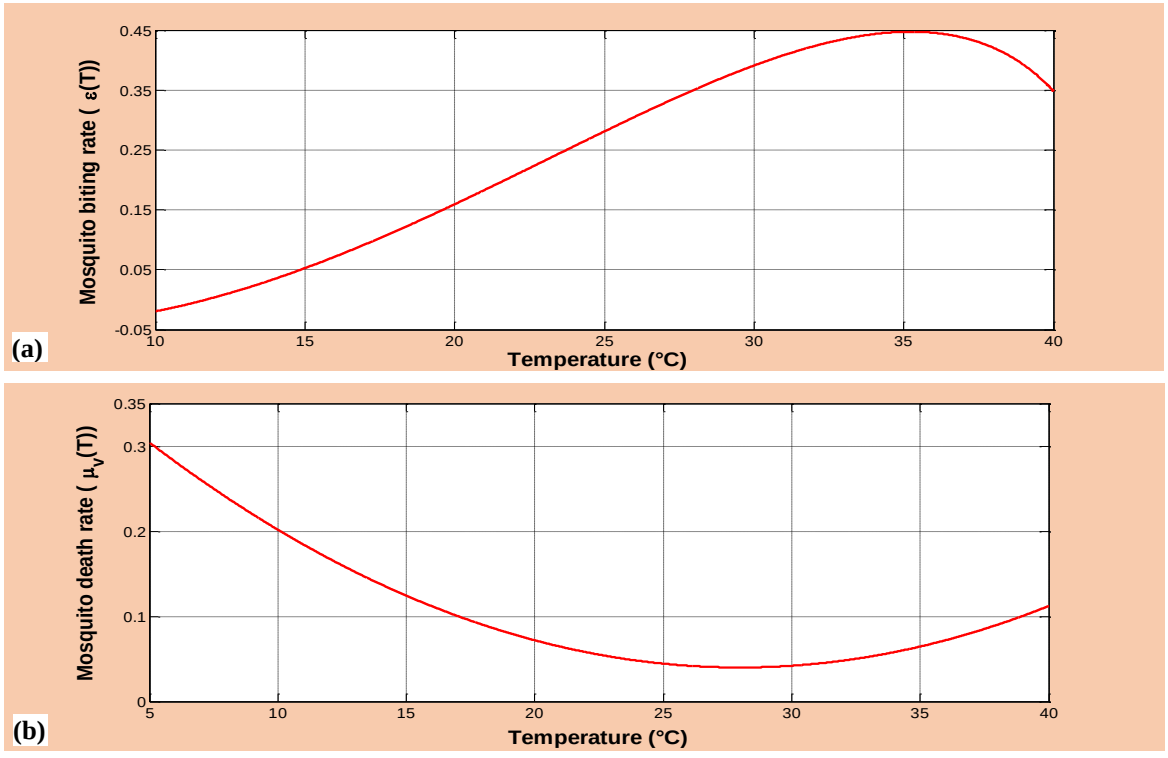

Figure 2: Simulation of **(a)** Mosquito biting rate $\epsilon(T)$; **(b)** Adult Mosquito death rate $\mu_v(T)$. The Figure 2a demonstrates low mosquito biting rate $\epsilon(T)$ at temperatures below 15°C, gradually increasing with a slight declination at upper thermal limit of 35°C. The Figure 2b explains in line with [2, 27], that the mosquito death

rate $\mu_v(T)$ is high at low temperature below 20℃, low between $20-35$℃ and increases at temperature beyond 35℃.

Where $p_j(T)$ and $q_j(R)$ account for the effect of temperature and rainfall, respectively, on the mortality rate for each aquatic stage $\mu_j(T,R)$.

The temperature-dependent functions $u_b(T), g_j(T)\ and\ p_j(T)$ are defined, respectively, as

$$\begin{cases} u_b(T) = e^{-a_b(T-T_b)^2} \\ g_j(T) = e^{-a_j\left(T-T_j\right)^2} \\ p_j(T) = c_j\left(T-T_j^*\right)^2 + d_j \end{cases} \tag{29}$$

where the parameters $a_b, c_v\ and\ c_j$ specify the amplitude of the functions $u_b(T)$, $g_j(T)\ and\ p_j(T)$, respectively (these parameters can be determined using mosquito surveillance and weather data). Moreover, d_j is the minimum value of the function $p_j(T)$. Furthermore, T_b, T_j are the temperature values that correspond to the maximum value of $u_b(T)\ and\ g_j(T)$, respectively, and T_j^* is the temperature values that correspond to the minimum value of $p_j(T)$.

To capture the effects of rainfall as described above, the following functional forms for $v_b(R)$, $h_j(R)$ and $q_j(R)$ are derived:

$$\begin{cases} v_b(R) = \frac{(1+s_b)e^{-r_b\left(R-R_b\right)^2}}{e^{-r_b\left(R-R_b\right)^2}+s_b} \\ h_j(R) = \frac{(1+s_j)e^{-r_j\left(R-R_j\right)^2}}{e^{-r_j\left(R-R_j\right)^2}+s_j} \\ q_j(R) = 1+\frac{e_jR}{1+R} \end{cases} \tag{30}$$

where $r_b, s_b, s_b, r_j\ and\ e_j$ are parameters that specify the amplitude of the functions $v_b(R)$, $h_j(R)\ and\ q_j(R)$, respectively. Furthermore, R_j is the rainfall value that corresponds to the maximum value of $h_j(R)$. Most of the functions given by Equations (29) and (30) are illustrated in Figure 3.

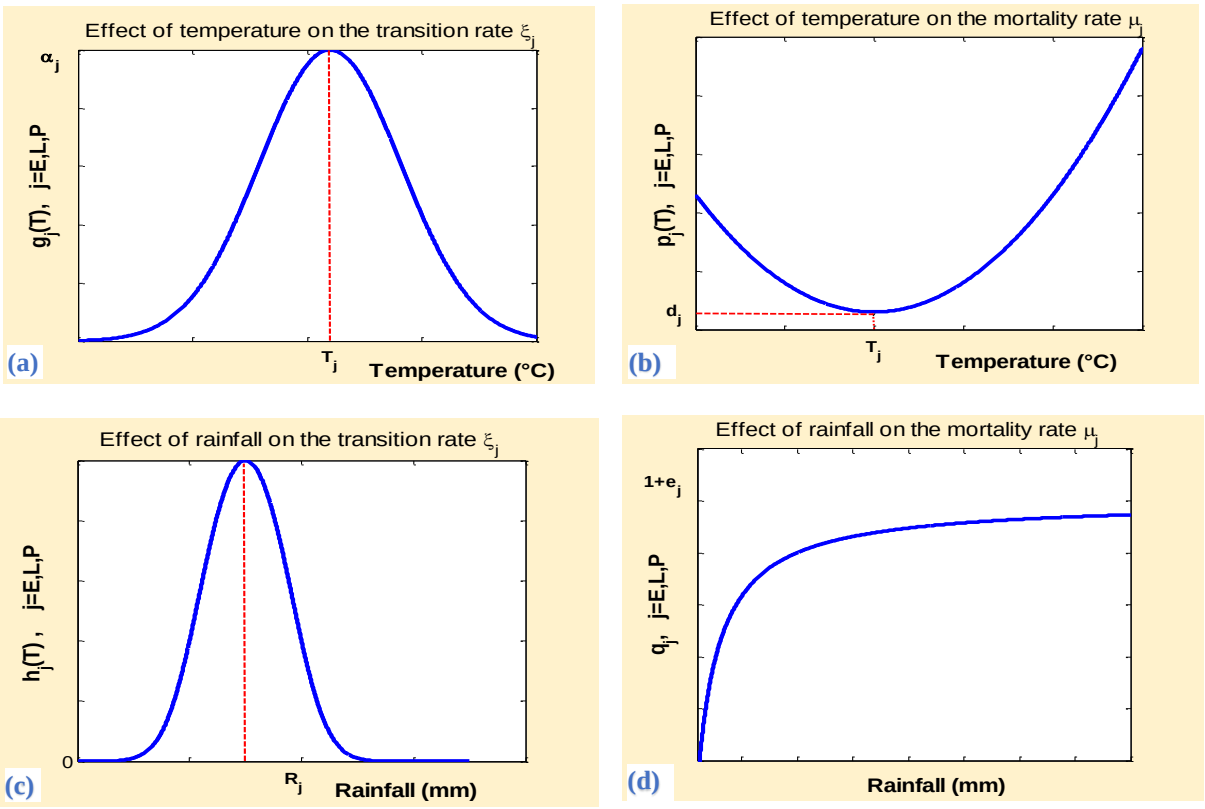

Figure 3: Plots of the temperature- and rainfall-dependent functions of the model (1) to (10)

The Figure 3a and Figure 3b show that how Temperature drives the mortality and transition rates functions in two different ways: higher temperatures favour higher transition rates between stages as shown in Figure 3a, although mortality rates decrease with temperature as shown in Figure 3b. The Figure 3c and Figure 3d also indicate that the transition and survivor probability of immature mosquitoes could be reduced by low or excessive levels of rainfall. Excessive levels of rainfall will flushed out the immature mosquitoes from their breeding site.

4. Numerical simulations

We compile two reasonable sets of baseline values for the parameters in the model: one for high risk areas and one for low risk areas of Ethiopia as shown in Table 6. We compute the sensitivity indices of the reproductive number to the parameters around these baseline values. The sensitivity indices allow us to compare the effectiveness of different control strategies, as each strategy affects different parameters to different degrees. We estimate parameter values from the country- and world-wide data and from published studies. We also analyze the sensitivity of the reproduction number and the state variables to the climatic variables.

4.1. Baseline parameter values

In 2017, the Ethiopia Federal Ministry of Health (FMOH) updated the country's malaria risk strata based upon malaria API (Annual Parasite Incidence), calculated from micro-plan data from more than 800 districts. A malaria risk map from this API analysis is shown in Figure 4, showing areas with malaria transmission risk by

API classified as High, Medium, Low, and Malaria-Free. Based on the current stratification, the proportion of the population at risk of malaria is about 60 percent [18, 19]. Our numerical analysis of the model considers these population at risk by classifying in to High risk area in which 3.4% of the population live, greater than 100 cases per 1000 people annually recorded and it is below 1750 meter above sea level; and Low risk areas in which 57.4% of the population live (Medium + Low), less than 100 cases per 1000 people annually recorded and it is above 1750 meter above sea level, for Ethiopia. The rest nearly 40% of Ethiopian people which we do not considered lives in malaria free risk areas [3, 19].

Table 2: Human population data for Ethiopia in 2017

Data Type	Total	At Risk	High risk	Low Risk	Sources
Number of people	104,957,434	63809550	3513264	60296286	[35, 36]
Birth (per 1000 population)	32.775	32.775	32.775	32.775	[14]
Life expectancy (years)	65	65	65	65	[14]
Estimated Malaria Case	2,658,314	2301600	962540	1339060	[35, 36]
Estimated Malaria Death	5352	4635	1938	2697	[35, 36]
No of people protected by ITNs or IRS	---	32%	32%	32%	[18, 36]

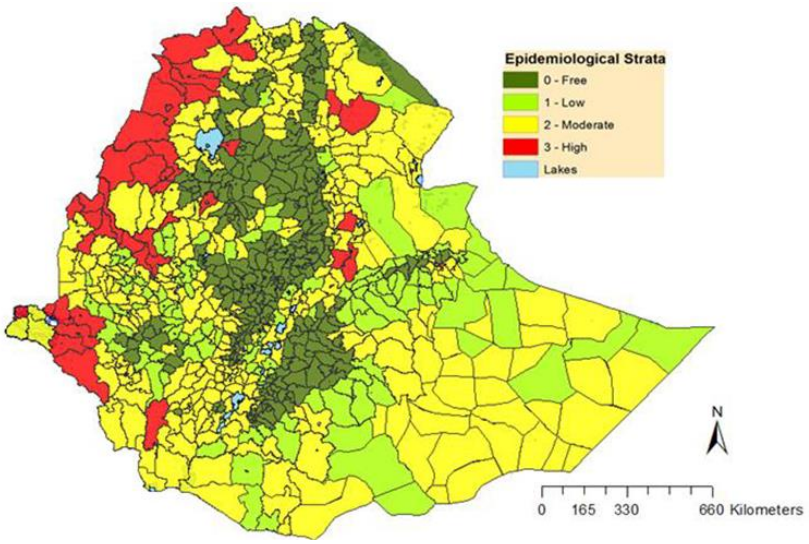

Figure 4: Malaria risk map of districts categorized by annual parasite incidence, Ethiopia, 2017.

In order to determine the values of the climate dependent parameters we use the average mean temperature and rainfall values (during mosquito season) of the corresponding districts of the total of more than 800 districts [19, 15]. The average monthly mean temperature (in °C) and rainfall (in mm) data from two groups of districts: one from high risk areas and one from low risk areas of Ethiopia [19, 15] is given in Table 3 and Table 4. Based on these data we obtained the mean temperature value of 25.04℃ and mean rainfall value (during mosquito season) of 10.67mm for high risk areas and the mean temperature value of 21.6℃ and mean rainfall value (during mosquito season) of 14mm for low risk areas of Ethiopia. Therefore, the temperature-dependent mosquito biting rate $\epsilon(T)$ and adult mosquito mortality rate $\mu_v(T)$ and all the temperature-and rainfall-

dependent parameters of aquatic stages, have been calculated with these temperature and rainfall values for both high and low risk areas of Ethiopia.

Table 3: Monthly mean temperature (in °C) and rainfall (in mm) for High Risk Areas of Ethiopia

Month	Jul	Aug	Sept	Oct	Nov	Dec	Jan	Feb	Mar	Apr	May	Jun
Temperature (°C)	23	23.1	24.2	24.2	24.4	24.7	23.8	26.9	27.2	27.5	26.6	24.9
Rainfall (mm)	113	229	212	167	5.9	0.75	5.15	6.5	18.3	27.4	221	311

Table 4: Monthly mean temperature (in °C) and rainfall (in mm) for Low Risk Areas of Ethiopia

Month	Jul	Aug	Sept	Oct	Nov	Dec	Jan	Feb	Mar	Apr	May	Jun
Temperature (°C)	20.7	20.6	20.8	20.7	19.6	19.2	20	22.3	23.8	24.4	24	23.1
Rainfall (mm)	352	289	155	70	4.8	2	2	34.5	15.8	24.9	120.4	33.5

We used the formulae given in equations (24), (25), (26), (27), (28) with some fixed values of the parameters defined in Equations (29) and (30) for female mosquito taken from different published studies as follows:

Table 5: Values of the parameters defined in Equations (29) and (30) for female mosquito.

Parameter	Value	Reference	Parameter	Value	Reference
$\boldsymbol{\alpha_b}$	200 day^{-1}	[30]	a_e	0.011 day^{-1}	[1]
$\boldsymbol{\alpha_e}$	0.5 day^{-1}	[1]	a_l	0.013 day^{-1}	[1]
$\boldsymbol{\alpha_l}$	0.35 day^{-1}	[1]	a_p	0.014 day^{-1}	[1]
$\boldsymbol{\alpha_p}$	0.5 day^{-1}	[1]	e_e	0.98 day^{-1}	[30]
$\boldsymbol{T_e^*}$	20 ℃	[33]	e_l	1.1 day^{-1}	[1]
$\boldsymbol{T_l^*}$	20 ℃	[33]	e_p	1.1 day^{-1}	[1]
$\boldsymbol{T_p^*}$	20 ℃	[33]	s_b	1.2 day^{-1}	[1]
$\boldsymbol{T_b}$	22 ℃	[33]	s_e	1.5 day^{-1}	[1]
$\boldsymbol{T_e}$	22 ℃	[33]	s_l	1.5 day^{-1}	[1]
$\boldsymbol{T_l}$	22 ℃	[33]	s_p	1.5 day^{-1}	[1]
$\boldsymbol{T_p}$	22 ℃	[33]	r_b	0.05 day^{-1}	[1]
$\boldsymbol{c_e}$	0.001 day^{-1}	[1]	r_e	0.05 day^{-1}	[1]
$\boldsymbol{c_l}$	0.0025 day^{-1}	[1]	r_l	0.05 day^{-1}	[1]
$\boldsymbol{c_p}$	0.001 day^{-1}	[1]	r_p	0.05 day^{-1}	[1]
$\boldsymbol{d_e}$	0.15 day^{-1}	[12]	R_b	10 mm	[1]
$\boldsymbol{d_l}$	0.2 day^{-1}	[12]	R_e	15 mm	[33]
$\boldsymbol{d_p}$	0.15 day^{-1}	[12]	R_l	15 mm	[33]
$\boldsymbol{a_b}$	0.015 day^{-1}	[1]	R_p	15 mm	[33]

Thus, the basic and effective reproduction numbers of our model and the numerical values of the endemic equilibrium points for both high and low risk areas have been calculated based on these numerical values of the parameters. The numerical simulations and the sensitivity analysis of our model are also analyzed based on these numerical values of the parameters obtained and shown in Table 6.

Table 6: The initial values and the parameter estimations of the model (1) to (10).

Symbols	Descriptions	High Risk	Low Risk	Sources
$S_h(0)$	Initial value of Susceptible humans	1109180	38020996	[35, 36]
$P_h(0)$	Initial value of Protected humans	1124244	19294812	[23, 47]
$E_h(0)$	Initial value of Exposed humans	258650	820709	[35, 36]
$I_h(0)$	Initial value of Infectious humans	962540	1339060	[35, 36]
$R_h(0)$	Initial value of Recovered humans	58650	420709	[19, 36]
$E(0)$	Initial value of Eggs population	1500000	10000000	[6, 32]
$L(0)$	Initial value of Larvae population	250000	1000000	[6, 32]
$P(0)$	Initial value of Pupae population	70000	400000	[6, 32]
$S_v(0)$	Initial value of Susceptible female mosquitoes	200000	2000000	[27, 25]
$I_v(0)$	Initial value of Infectious female mosquitoes	20000	300000	[27, 25]
Parameter	**Descriptions**			
Λ	Constant recruitment rate for humans	321	5410	[35, 14]
γ	Proportion of new recruitments that are	0.32	0.32	[19, 36]
g	Transfer rate of humans from Susceptible to	0.00088	0.00088	[19, 36]
C_{vh}	Probability of transmission of infection from an infectious mosquito to a susceptible human	0.04	0.04	[2, 27]
η	Rate of progression of humans from the exposed state to the infectious state.	0.0714	0.0625	[4, 7]
τ	Natural recovery rate	0.0015	0.002	[25, 7]
α	Recovery rate due to treatment	0.001	0.0015	[25, 7]
δ	Rate of loss of immunity	0.00078	0.0014	[28]
φ	Proportions of humans who lose their immunity that become Susceptible.	0.68	0.68	[28]
f	Transfer rate of humans from Protected to	0.002	0.002	[19, 36]
μ_h	Natural mortality rate for humans	0.000043	0.000043	[14]
μ_d	Disease-induced mortality rate for humans.	0.000006	0.000006	[35, 36]
C_{hv}	Probability of transmission of infection from an infectious human to a susceptible mosquito.	0.83	0.48	[25, 8]
$\widetilde{C}_{hv}$	Probability of transmission of infection from a recovered human to a susceptible mosquito.	0.083	0.048	[25, 8]
K_E	The Eggs Carrying capacity	10^7	10^8	[2, 8]
K_L	The Larvae Carrying capacity	$2.0 * 10^6$	$2.4 * 10^7$	[27, 25]
$\epsilon(T)$	The mosquito biting rate	0.3	0.2	[2, 24, 27]
$\mu_v(T)$	Natural mortality rate for female mosquitoes	0.0444	0.0605	[1]
$b(T,R)$	Eggs oviposition rate	172	120	[19, 15]
$\xi_e(T,R)$	Hatching rate of eggs	0.2338	0.4842	[19, 15]
$\xi_l(T,R)$	Development rate of larvae into pupae	0.1606	0.3388	[19, 15]
$\xi_p(T,R)$	Development rate of pupae into adult	0.2274	0.4797	[19, 15]
$\mu_e(T,R)$	Natural mortality rate of eggs	0.3326	0.2921	[19, 15]
$\mu_l(T,R)$	Natural mortality rate of larvae	0.4996	0.3952	[19, 15]
$\mu_p(T,R)$	Natural mortality rate of pupae	0.2378	0.1964	[19, 15]

We take the initial conditions from the data of Ministry of Health (MoH) of Ethiopia and from the data of World Health Organization (WHO) about Ethiopia and is also shown in Table 6.

4.2. Derived quantities

In this section, we found the numerical value of effective reproductive number $\mathcal{R}_{eff}$ and the endemic equilibrium point $\mathcal{E}^*$ for the malaria model (1) to (10) for the baseline parameter values given in Table 6.

4.2.1. High risk areas

For the baseline parameters for high risk areas malaria transmission the effective reproductive number, $\mathcal{R}_{eff} = 2.6818$. There is only one endemic equilibrium point, $\mathcal{E}^*$ shown in Table 7. since $\mathcal{R}_{eff} > 1$. We show a numerical simulation of the malaria model (1) to (10) in Figure 5. which shows that the system approaches the endemic equilibrium point given in Table 7.

Table 7: The endemic equilibrium point for the malaria model (1) to (10) for the baseline parameter values described in Table 6 for the transmission of high-risk areas of $\mathcal{R}_{eff} > 1$.

$S_h(t) = 1.4865 \times 10^6$	$E(t) = 9.8556 \times 10^6$
$P_h(t) = 1.1187 \times 10^6$	$L(t) = 1.2714 \times 10^6$
$E_h(t) = 4.1183 \times 10^4$	$P(t) = 4.3893 \times 10^5$
$I_h(t) = 1.1536 \times 10^6$	$S_v(t) = 1.0433 \times 10^6$
$R_h(t) = 3.5042 \times 10^6$	$I_v(t) = 1.2048 \times 10^6$

4.2.2. Low risk areas

For the baseline parameters for low risk areas malaria transmission the effective reproductive number, $\mathcal{R}_{eff} = 1.3074$. There is only one endemic equilibrium point, $\mathcal{E}^*$ shown in Table 8, since $\mathcal{R}_{eff} > 1$. We show a numerical simulation of the malaria model (1) to (10) in Figure 6 which shows that the system approaches the endemic equilibrium point given in Table 8.

Table 8: The endemic equilibrium for the malaria model (1) to (10) for the baseline parameter values described in Table 6 for the transmission of low-risk areas of $\mathcal{R}_{eff} > 1$.

$S_h(t) = 5.7970 \times 10^7$	$E(t) = 9.9081 \times 10^7$
$P_h(t) = 3.1199 \times 10^7$	$L(t) = 1.7554 \times 10^7$
$E_h(t) = 5.7453 \times 10^5$	$P(t) = 1.2027 \times 10^7$
$I_h(t) = 1.0118 \times 10^7$	$S_v(t) = 6.0109 \times 10^7$
$R_h(t) = 2.4541 \times 10^7$	$I_v(t) = 9.6389 \times 10^6$

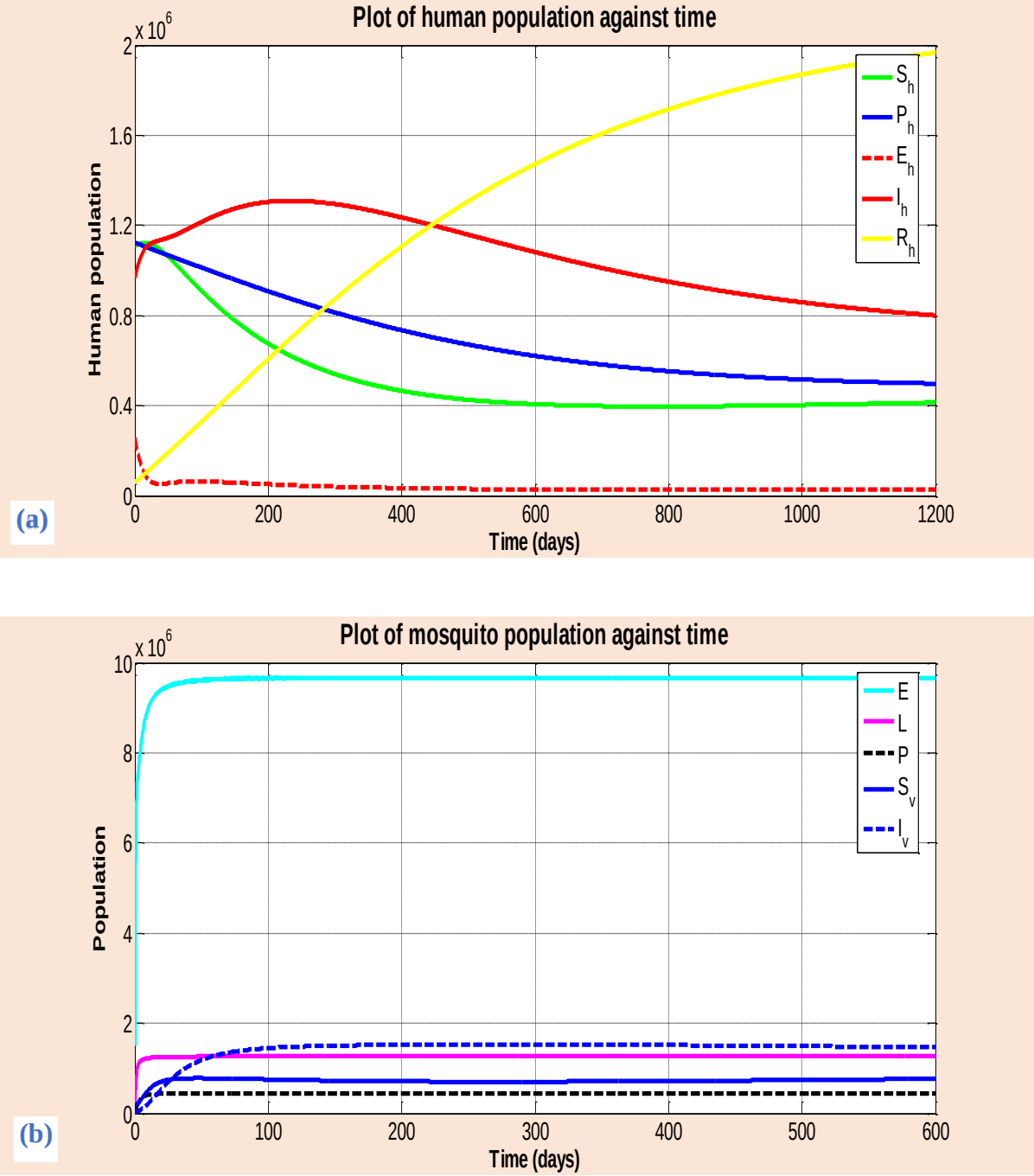

Figure 5: A numerical simulation of the malaria model (1) to (10) with baseline parameter values defined in Table 6 for areas of high-risk transmission. These parameters correspond to $\mathcal{R}_{eff} = 2.6818$. The initial conditions used are also given in Table 6. The system approaches the endemic equilibrium point given in Table 7. The simulations were conducted using MATLAB's ode45.

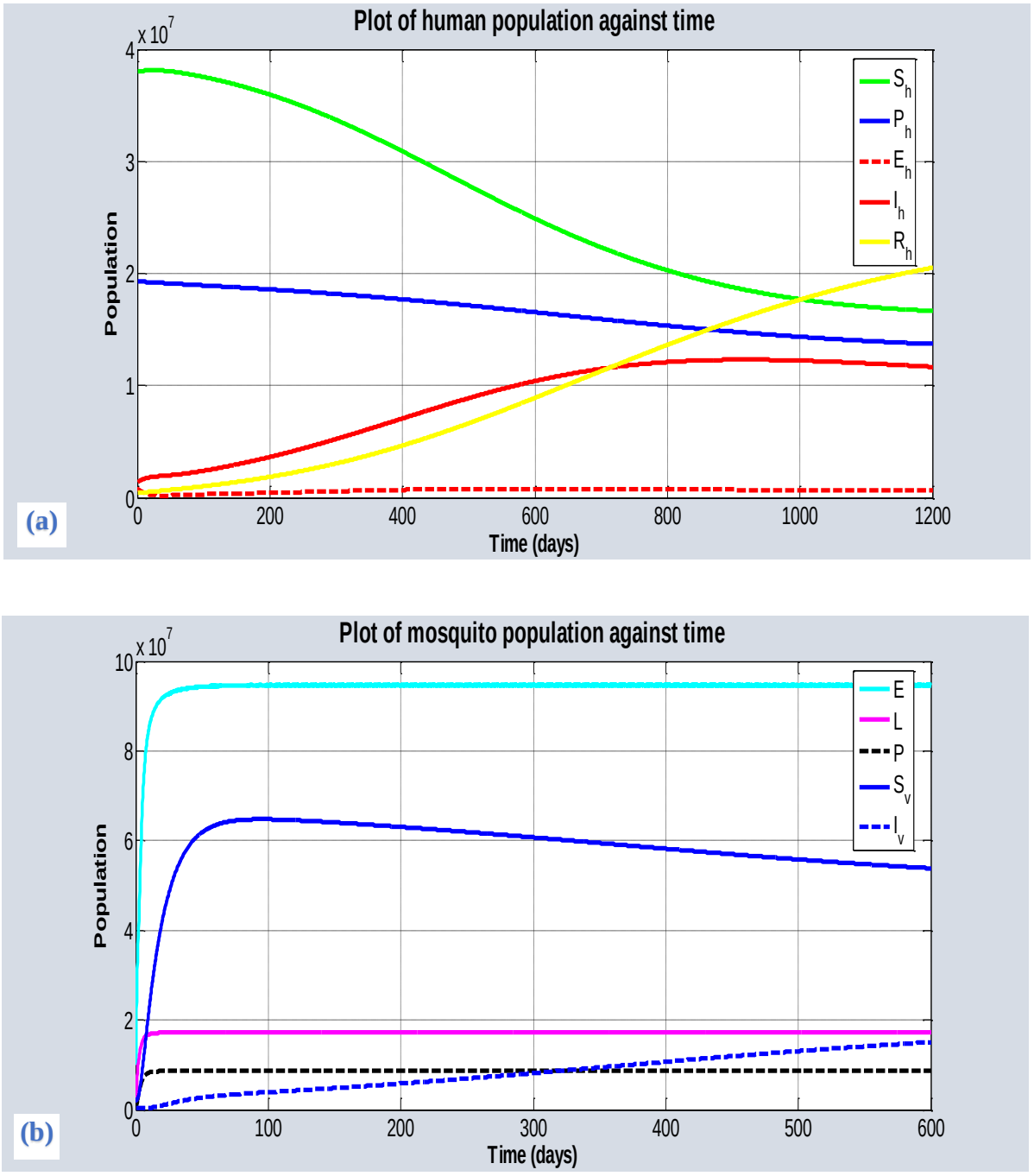

Figure 6: A numerical simulation of the malaria model (1) to (10) with baseline parameter values defined in Table 6 for areas of low risk transmission. These parameters correspond to $\mathcal{R}_{eff} = 1.3074$. The initial conditions used are also given in Table 6. The system approaches the endemic equilibrium point given in Table 8. The simulations were conducted using MATLAB's ode45.

4.3. Sensitivity analysis

The normalized forward sensitivity index of a variable $\mathcal{R}_{eff}$ that depends differentiably on a parameter p is defined as:

$SI_p^{\mathcal{R}_{eff}} = \frac{\partial \mathcal{R}_{eff}}{\partial p} * \frac{p}{\mathcal{R}_{eff}}$.

Table 9: Sensitivity indices of $\mathcal{R}_{eff}$ to parameters for the malaria model (1) to (10), evaluated at the baseline parameter values given in Table 6. The parameters are ordered from most sensitive to least.

High Risk Area				**Low Risk Area**			
	Parameter	Sign	Value		Parameter	Sign	Value
1	$\epsilon(T)$	+	1.0	1	$\epsilon(T)$	+	1.0
2	$\mu_v(T)$	−	0.9974	2	$\mu_v(T)$	−	0.9988
3	C_{vh}	+	0.5000	3	C_{vh}	+	0.5000
4	Λ	−	0.5000	4	Λ	−	0.5000
5	μ_h	+	0.4850	5	μ_h	+	0.4950
6	$\xi_l(T,R)$	+	0.4581	6	$\xi_l(T,R)$	+	0.4391
7	C_{hv}	+	0.3835	7	C_{hv}	+	0.4024
8	K_L	+	0.3195	8	K_L	+	0.3666
9	$\xi_p(T,R)$	+	0.2569	9	τ	−	0.2260
10	τ	−	0.2243	10	g	−	0.2200
11	g	−	0.2200	11	α	−	0.1695
12	K_E	+	0.1805	12	f	+	0.1507
13	$\xi_e(T,R)$	+	0.1786	13	$\xi_p(T,R)$	+	0.1456
14	$\mu_p(T,R)$	−	0.1750	14	K_E	+	0.1334
15	f	+	0.1507	15	$\xi_e(T,R)$	+	0.1320
16	α	−	0.1496	16	$\tilde{C}_{hv}$	+	0.0976
17	$\mu_l(T,R)$	−	0.1442	17	δ	−	0.0947
18	$\tilde{C}_{hv}$	+	0.1165	18	$\mu_l(T,R)$	−	0.0731
19	δ	−	0.1104	19	$\mu_p(T,R)$	−	0.0154
20	γ	−	0.0068	20	γ	−	0.0068
21	$b(T,R)$	+	0.0026	21	$b(T,R)$	+	0.0012
22	$\mu_e(T,R)$	−	0.0016	22	μ_d	−	0.0008
23	μ_d	−	0.0012	23	$\mu_e(T,R)$	−	0.0005
24	η	−	0.0003	24	η	−	0.0003

In the next section we will discuss some of the relationship between the effective reproduction number and the parameters using graphs which shows changes of parameters and their effects on $\boldsymbol{\mathcal{R}_{eff}}$ as follows:

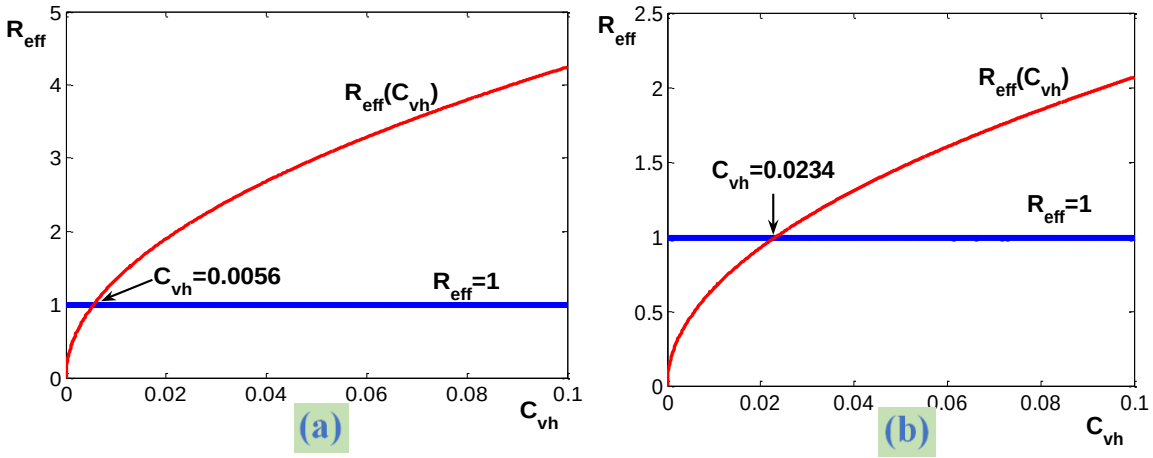

Figure 7: Graphs of the effective reproduction number $\mathcal{R}_{eff}$ versus the probability of transmission of the disease from an infectious mosquito to a susceptible human C_{vh}. **(a)** for high risk areas **(b)** for low risk areas.

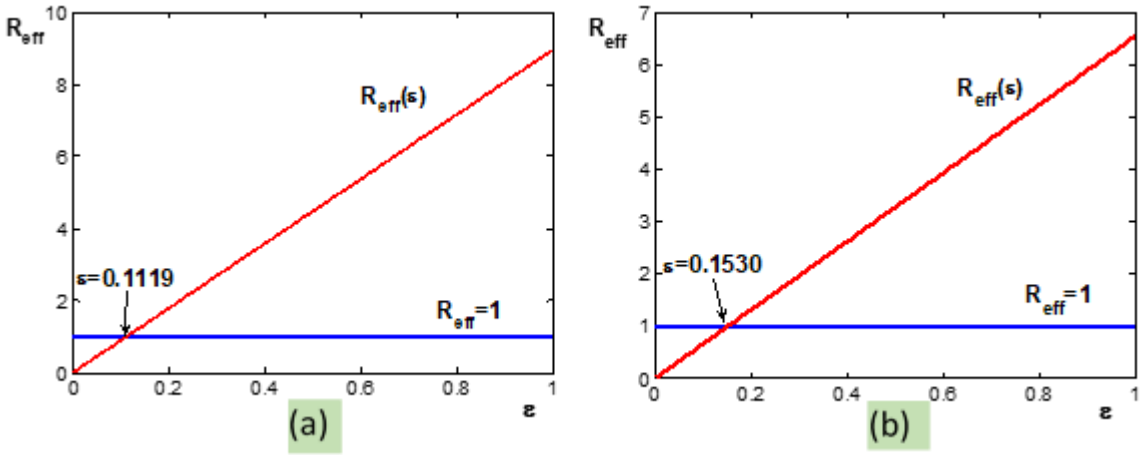

Figure 8: Graphs of the effective reproduction number $\mathcal{R}_{eff}$ versus mosquito biting rate $\in (T)$ **(a)** for high risk areas **(b)** for low risk areas.

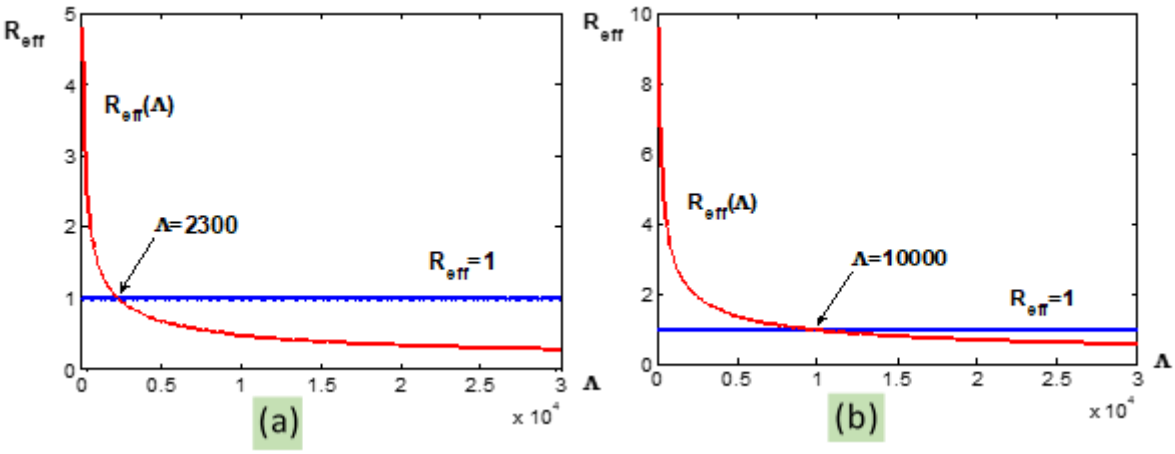

Figure 9: Graphs of the effective reproduction number $\mathcal{R}_{eff}$ versus the recruitment rate for humans Λ. **(a)** for high risk areas **(b)** for low risk areas.

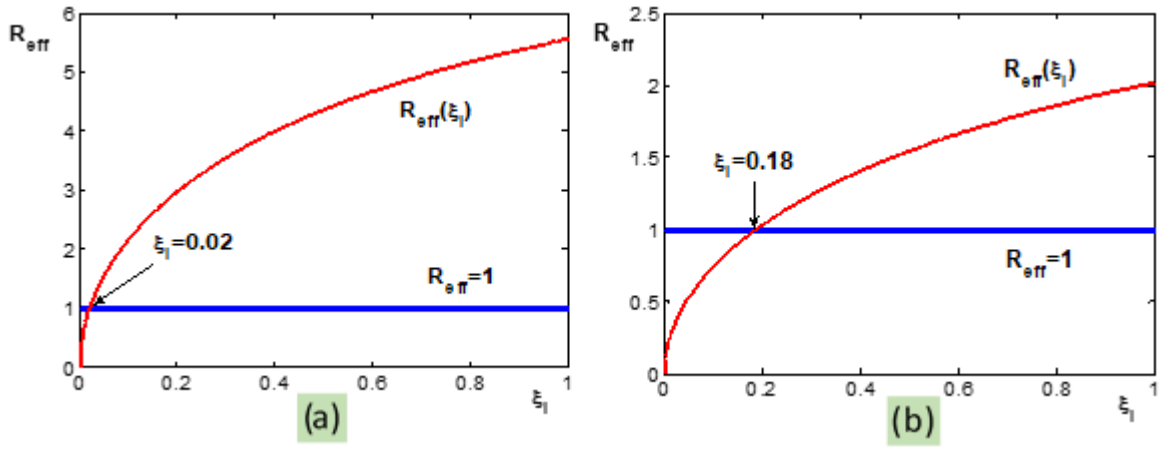

Figure 10: Graphs of the effective reproduction number $\mathcal{R}_{eff}$ versus the Development rate of larvae into pupae ξ_l. **(a)** for high risk areas **(b)** for low risk areas.

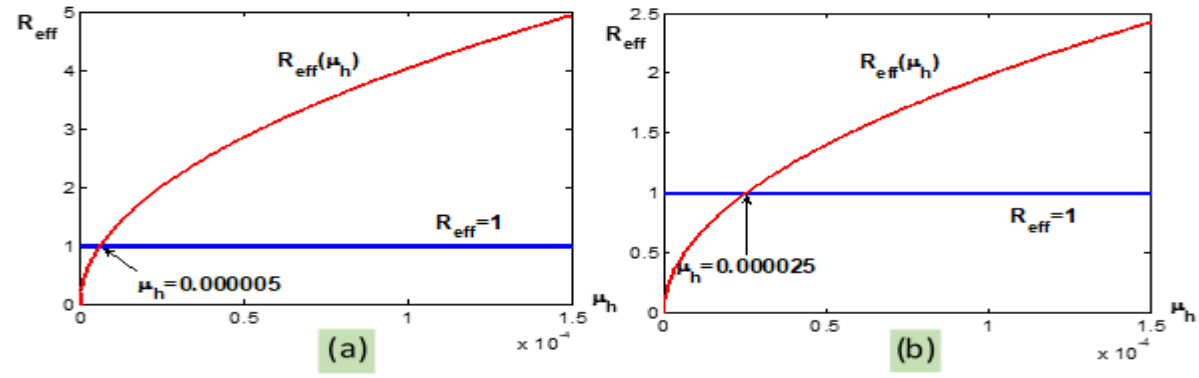

Figure 11: Graphs of the effective reproduction number $\mathcal{R}_{eff}$ versus the humans' natural mortality rate μ_h. **(a)** for high risk areas **(b)** for low risk areas.

Our model with a seasonal averaged climate values in two study areas is analyzed regarding malaria transmission as in [26]. For example, the investigated sensitivity of $\mathcal{R}_{eff}$ to the average monthly temperature and rainfall data given in Table 3 and 4 are presented in Table 10.

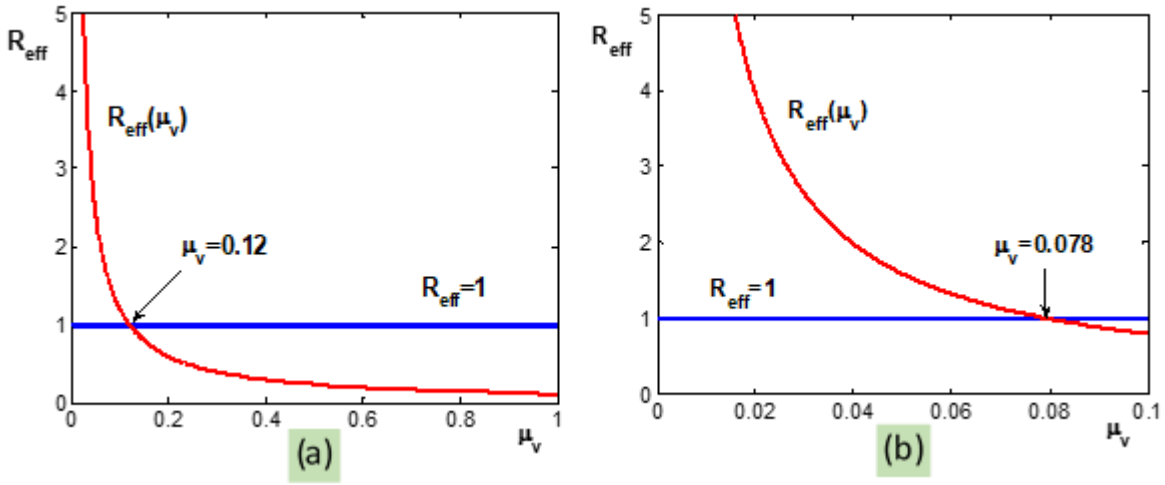

Figure 12: Graphs of the effective reproduction number $\mathcal{R}_{eff}$ versus the Natural mortality rate for adult female mosquitoes $\mu_v(T)$. **(a)** for high risk areas **(b)** for low risk areas.

Table 10: Estimate of effective reproduction number $\mathcal{R}_{eff}$ against Monthly Mean Rainfall (MR) and Mean Temperature (MT) of Ethiopia in 2017 using parameter values from Table 6.

Month	**High risk area**			**Low risk area**		
	MT (°C)	**MR (mm)**	$\mathcal{R}_{eff}$	**MT (°C)**	**MR (mm)**	$\mathcal{R}_{eff}$
Jul	23	113	2.67	20.7	352	0.84
Aug	23.1	229	2.72	20.6	289	0.83
Sept	24.2	212	3.14	20.8	155	0.86
Oct	24.2	167	3.14	20.7	70	0.84
Nov	24.4	5.9	2.41	19.6	4.8	0.75
Dec	24.7	0.75	2.47	19.2	2	0.67
Jan	23.8	5.15	2.27	20	2	0.85
Feb	26.9	6.5	2.47	22.3	34.5	1.6
Mar	27.2	18.3	2.42	23.8	15.8	1.94
Apr	27.5	27.4	2.35	24.4	24.9	2.1
May	26.6	221	3.38	24	120.4	1.59
Jun	24.9	311	3.33	23.1	33.5	1.74

5. Results and discussions

In this research work, we considered non-linear dynamical system to study the dynamics of a malaria disease in Ethiopia. The climatic factors such as temperature and rainfall are also considered in order to study their effect on the malaria disease transmission. We found the effective reproduction number for high risk areas of Ethiopia as $\mathcal{R}_{\text{eff}} = 2.6818$ and for low risk areas as $\mathcal{R}_{\text{eff}} = 1.3074$. In both cases $\mathcal{R}_{\text{eff}}$ is greater than one. We observe from the numerical simulation Figure 5 and Figure 6 that the stability of the endemic equilibrium point as the system converges to the endemic equilibrium point for $\mathcal{R}_{\text{eff}} > 1$ in both areas. We have also evaluated the sensitivity indices at the baseline parameter values given in Table 6. In both cases, of high and low risk areas of transmission, the most sensitive parameters are the mosquito biting rate $\epsilon(\mathrm{T})$, and adult female mosquito mortality rate $\mu_{\mathrm{v}}(\mathrm{T})$, both are temperature dependent parameters. Other important parameters include the probability of disease transmission from infectious mosquitoes to susceptible humans C_{vh}, the humans recruitment rate Λ, the humans natural mortality rate μ_{h}, the larvae development rate $\xi_{\mathrm{l}}(\mathrm{T},\mathrm{R})$ which depends on both temperature and rainfall. From Figure 8, we observed that an increase in the mosquito biting rate $\epsilon(\mathrm{T})$, makes an increase the effective reproduction number $\mathcal{R}_{\text{eff}}$. When $\epsilon(\mathrm{T})$ is less than 0.1119 for high risk and less than 0.1530 for low risk areas then $\mathcal{R}_{\text{eff}} < 1$ which tell us, the disease does not spread. Whereas, when $\epsilon(\mathrm{T})$, is greater than 0.1119 for high risk and greater than 0.1530 for low risk areas, makes $\mathcal{R}_{\text{eff}} > 1$ and tell us the disease persists/spreads in the community. From figure 12, we can observe that when the mortality rate for mosquitoes $\mu_{\mathrm{v}}(\mathrm{T})$ is less than 0.12 for high risk and less than 0.078 for low risk areas, then the reproduction number $\mathcal{R}_{\text{eff}} > 1$ and this tell us the disease persists/spreads in the community. Whereas, when the value of $\mu_{\mathrm{v}}(\mathrm{T})$ is greater than 0.12 for high risk and greater than 0.078 for low risk areas, then the reproduction number $\mathcal{R}_{\text{eff}} < 1$ this means that the spread of malaria disease decreases in the community. The Figure 2a demonstrates low mosquito biting rate at temperatures below $15℃$, gradually increasing with a slight declination at upper thermal limit of $35℃$. The Figure 2b explains that the mosquito death rate is high at low temperature below $20℃$, low between $20 - 35℃$ and increases at temperature beyond $35℃$. This shows the significant role of warmer temperatures in the aggravation of the disease. As the temperature is greater in high risk areas than in low risk areas, relatively there is high mosquito biting rate and low mortality rate in high risk areas than low risk areas. This results on the greater effective reproduction number $\mathcal{R}_{\text{eff}} = 2.6818$ for high risk areas than the effective reproduction number $\mathcal{R}_{\text{eff}} = 1.3074$ for low risk areas. The results in these both regions indicate that malaria trend follows the climate pattern. Furthermore, one of the six most sensitive parameters is also the larvae development rate $\xi_{\mathrm{l}}(\mathrm{T},\mathrm{R})$ which is dependent of both temperature and rainfall. So that for the immature mosquitoes, eggs, larvae and pupae, in addition to the temperature, the rainfall is an important factor. Our results in Table 10 indicate that R_{eff} varies in the year with the influence of rainfall and temperature. We note in the results that the effective reproduction number value increases especially before and after the peak period of the rainy season starting from May to June and from September to October in high risk areas. In low risk areas the transmission also increases during February to June but with low disease intensity compared to high risk areas which is most likely owing to the climate differences. The result also confirms that malaria transmission is influenced by weather and rainfall, since the disease is more prevalent in the favorable climate of high-risk areas than it is in low risk areas. In our model the intervention coverages are incorporated, by considering the protected human compartment which consists of people who are protected either by ITNs or IRS, and showed

that the reproduction number is reduced in both high and low risk areas. For example, in high risk areas if there is no any intervention the effective reproduction number $\mathcal{R}_{\text{eff}} = 2.6818$ would be increased to $\mathcal{R}_0 = 3.2204$ which is called the basic reproduction number. Similarly, in low risk areas if there is no any intervention the effective reproduction number $\mathcal{R}_{\text{eff}} = 1.3074$ would be increased to $\mathcal{R}_0 = 1.5718$. In the absence of any intervention, we note a large number of $\mathcal{R}_{\text{eff}}$, confirming a substantial increase in incidence of malaria in the community.

6. Conclusions and recommendations

6.1. Conclusions

In this study, we first showed that there exists a feasible region Γ where the model has a positive and bounded solution. We showed the existence of the disease-free equilibrium point $\mathcal{E}_0$ and the endemic equilibrium point $\mathcal{E}^*$ of the model. Then we have found the effective reproduction number $\mathcal{R}_{eff}$ and we showed that, if $\mathcal{R}_{eff} < 1$ then the disease-free equilibrium point, $\mathcal{E}_0$ is locally as well as globally asymptotically stable; and if $\mathcal{R}_{eff} > 1$ then $\mathcal{E}_0$ is unstable. We also proved that a unique endemic equilibrium point $\mathcal{E}^*$ exists and is locally as well as globally asymptotically stable for all $\mathcal{R}_{eff} > 1$. The numerical simulation of the model is derived from the data representing two risk areas of Ethiopia collected from the country- and world- wide sources. In both cases the effective reproduction number obtained is greater than one. This in principle implies that one infectious individual infects more than two healthy individuals in high risk areas and more than one healthy individual in low risk areas in his/her infectious time; which shows that the disease spreads in the population. From the most sensitive parameters $\epsilon(\mathrm{T})$ and $\mu_v(\mathrm{T})$, both are temperature dependent parameters, we can conclude that in order to control malaria transmissions more emphasis should be given to these parameters especially during the temperature of high effect. Difference of the effective reproduction number values of high and low risk areas are also indicate that $\mathcal{R}_{\text{eff}}$ is sensitive to the climate differences, since the disease is more prevalent in the favorable climate of high-risk areas than it is in low risk areas. The parameters related with the immature mosquito dynamics like the larvae development rate ξ_l are also highly sensitive to the model. Finally, the results indicate that implementing the interventions like insecticide treated nets (ITNs), and indoor residual spray (IRS) help to control the parameters sensitive to the reproduction number and hence protect the people from the disease. Especially these interventions should be implemented mostly between February and June when the climatic conditions are favorable for mosquitoes' development in low risk areas and throughout the year in high risk areas of Ethiopia. However, there are other factors which need to be considered in studying malaria transmission. Some of these factors include; influence of humidity on the dynamics of the vector population, emigration and migration of humans, economic development and so on. We leave these aspects and the bifurcation analysis of the model for future studies.

6.2. Recommendations

From the above results and discussion, we would like to recommend the following to control the spread of malaria in Ethiopia: One of the most sensitive parameters of our model is the mosquito biting rate $\epsilon(\mathrm{T})$, so it is reasonable to recommend the use of ITNs as intervention strategy for malaria transmission in making $\epsilon(\mathrm{T})$ less than 0.1119 for high risk areas and less than 0.1530 for low risk areas of Ethiopia. The proportion of ITN

coverage, individual's exposedness to mosquito bites, and the effectiveness of the bed nets should be targeted by the stakeholders. The other sensitive parameter of our model is the adult female mosquito mortality rate $\mu_v(T)$, it should be greater than 0.12 for high risk areas and greater than 0.078 for low risk areas, so the use of IRS is recommended to increase $\mu_v(T)$. In order to reduce the disease transmission $\mathcal{R}_{eff}$ in Ethiopia; the probability of disease transmission from infectious mosquitoes to susceptible humans C_{vh} should be less than 0.0056 for high risk areas and less than 0.0234 for low risk areas. We can also suggest that destruction of mosquitoes breeding sites and regular use of larvicides have high potential to reduce malaria transmission by reducing the development rate of larvae ξ_l to less than 0.02 for high risk areas and less than 0.18 for low risk areas. In order to keep the country from the climate negative impact on the malaria transmission the interventions should be implemented especially between February and June when the climatic conditions are favorable for mosquitoes' development in low risk and throughout the year in high risk areas of Ethiopia when the $\mathcal{R}_{eff}$ increases as shown in Table 10.

7. Limitations of the study

There was lack of whether and surveillance data regarding to the mosquito population in the mature and immature stages.

Reference

[1]. Abdelrazec A, Gumel AB. Mathematical assessment of the role of temperature and rainfall on mosquito population dynamics. Journal of mathematical biology. 2017 May 1;74(6):1351-95.

[2]. Abiodun GJ, Witbooi P, Okosun KO. Modelling the impact of climatic variables on malaria transmission. Hacettepe journal of mathematics and statistics. 2018 Apr 1;47(2):219-35.

[3]. Alelign A, Dejene T. Current status of malaria in Ethiopia: evaluation of the burden, factors for transmission and prevention methods. Acta Parasitologica Globalis. 2016;7(1):01-6.

[4]. Anderson RM, May RM. Infectious diseases of humans: dynamics and control. Oxford university press; 1992 Aug 27.

[5]. Aron JL, May RM. The population dynamics of malaria. In The population dynamics of infectious diseases: theory and applications 1982 (pp. 139-179). Springer, Boston, MA.

[6]. Bakary T, Boureima S, Sado T. A mathematical model of malaria transmission in a periodic environment. Journal of biological dynamics. 2018 Jan 1;12(1):400-32.

[7]. Chitnis NR. Using mathematical models in controlling the spread of malaria.

[8]. Chiyaka C, Tchuenche JM, Garira W, Dube S. A mathematical analysis of the effects of control strategies on the transmission dynamics of malaria. Applied Mathematics and Computation. 2008 Feb 1;195(2):641-62.

[9]. Deribew A, Dejene T, Kebede B, Tessema GA, Melaku YA, Misganaw A, et al. Incidence, prevalence and mortality rates of malaria in Ethiopia from 1990 to 2015: analysis of the global burden of diseases 2015. Malaria journal. 2017 Dec;16(1):271.

[10]. Diekmann O., Heesterbeek J. A and Metz J. A., On the definition and computation of R_0 in the model for infectious disease in heterogeneous population. Journal of mathematical Biology, 28 (1990), 365-

382.

[11]. Girum T, Shumbej T, Shewangizaw M. Burden of malaria in Ethiopia, 2000-2016: findings from the Global Health Estimates 2016. Tropical Diseases, Travel Medicine and Vaccines. 2019 Dec 1;5(1):11.

[12]. Hilker FM, Westerhoff FH. Preventing extinction and outbreaks in chaotic populations. The American Naturalist. 2007 Aug;170(2):232-41.

[13]. http://www.malwest.gr/en-us/malaria/informationforhealthcareprofessionals/Plasmodiumlifecycle.aspx.

[14]. https://data.worldbank.org/indicator/SP.DYN.CDRT.IN?locations=ET

[15]. https://en.climate-data.org/africa/ethiopia-249/

[16]. https://en.wikipedia.org/wiki/Plasmodium#Life_cycle

[17]. https://www.cdc.gov/malaria/about/biology/index.html

[18]. https://www.pmi.gov/docs/default-source/default-document-library/malaria-operational-plans/fy-2018/fy-2018-ethiopia-malaria-operational-plan.pdf

[19]. https://www.pmi.gov/docs/default-source/default-document-library/malaria-operational-plans/fy19/fy-2019-ethiopia-malaria-operational-plan.pdf?sfvrsn=3

[20]. J. P. LaSalle, The Stability of Dynamical Systems, Regional Conference Series in Applied Mathematics, SIAM, Philadelphia, Pa, USA, 1976.

[21]. Koella JC. On the use of mathematical models of malaria transmission. Acta tropica. 1991 Apr 1;49(1):1-25.

[22]. MacDonald G. The epidemiology and control of malaria. London: Oxford Univ. Pr.

[23]. Mandal S, Sarkar RR, Sinha S. Mathematical models of malaria-a review. Malaria journal. 2011 Dec;10(1):202.

[24]. Martens WJ, Niessen LW, Rotmans J, Jetten TH, McMichael AJ. Potential impact of global climate change on malaria risk. Environmental health perspectives. 1995 May;103(5):458-64.

[25]. Mohammed-Awel J, Agusto F, Mickens RE, Gumel AB. Mathematical assessment of the role of vector insecticide resistance and feeding/resting behavior on malaria transmission dynamics: Optimal control analysis. Infectious Disease Modelling. 2018 Jan 1;3:301-21.

[26]. Mukhtar AY. Mathematical modeling of the transmission dynamics of malaria in South Sudan.

[27]. Ngarakana-Gwasira ET, Bhunu CP, Mashonjowa E. Assessing the impact of temperature on malaria transmission dynamics. Afrika Matematika. 2014 Dec 1;25(4):1095-112.

[28]. Okosun KO, Makinde OD. Modelling the impact of drug resistance in malaria transmission and its optimal control analysis. International Journal of Physical Sciences. 2011 Nov 9;6(28):6479-87.

[29]. P. van den Driessche and J. Watmough, “Reproduction numbers and sub-threshold endemic equilibria for compartmental models of disease transmission,” Mathematical Biosciences, vol. 180, no. 1-2, pp. 29–48, 2002.

[30]. Parham PE, Michael E. Modelling climate change and malaria transmission. In Modelling Parasite Transmission and Control 2010 (pp. 184-199). Springer, New York, NY.

[31]. Ross R. The prevention of malaria. John Murray; London; 1911.

[32]. Traoré B, Sangaré B, Traoré S. A mathematical model of malaria transmission with structured vector population and seasonality. Journal of Applied Mathematics. 2017 Jan 1;2017.

[33]. Turell MJ, Dohm DJ, Sardelis MR, O'guinn ML, Andreadis TG, Blow JA. An update on the potential of North American mosquitoes (Diptera: Culicidae) to transmit West Nile virus. Journal of medical entomology. 2005 Jan 1;42(1):57-62.

[34]. World Health Organization, 2018. World malaria report 2017. Geneva: World Health Organization.

[35]. World Health Organization. 2019. World malaria report 2018. Geneva: World Health Organization.

[36]. World Health Organization. 2020. World malaria report 2019. Geneva: World Health Organization.